

Light Quark Masses from Lattice QCD

Rajan Gupta¹ and Tanmoy Bhattacharya²

*Group T-8, Mail Stop B-285, Los Alamos National Laboratory
Los Alamos, NM 87545, U. S. A*

Abstract

We present estimates of the masses of light quarks using lattice data. Our main results are based on a global analysis of all the published data for Wilson, Sheikholeslami-Wohlert (clover), and staggered fermions, both in the quenched approximation and with $n_f = 2$ dynamical flavors. We find that the values of masses with the various formulations agree after extrapolation to the continuum limit for the $n_f = 0$ theory. Our best estimates, in the \overline{MS} scheme at $\mu = 2$ GeV, are $\overline{m} = 3.4 \pm 0.4 \pm 0.3$ MeV and $m_s = 100 \pm 21 \pm 10$ MeV in the quenched approximation. The $n_f = 2$ results, $\overline{m} = 2.7 \pm 0.3 \pm 0.3$ MeV and $m_s = 68 \pm 12 \pm 7$ MeV, are preliminary. (A linear extrapolation in n_f would further reduce these estimates for the physical case of three dynamical flavors.) These estimates are smaller than phenomenological estimates based on sum rules, but maintain the ratios predicted by chiral perturbation theory (χ PT). The new results have a significant impact on the extraction of ϵ'/ϵ from the Standard Model. Using the same lattice data we estimate the quark condensate using the Gell-Mann-Oakes-Renner relation. Again the three formulations give consistent results after extrapolation to $a = 0$, and the value turns out to be correspondingly larger, roughly preserving $m_s \langle \overline{\psi}\psi \rangle$.

15 April, 1997

¹Email: rajan@qcd.lanl.gov

²Email: tanmoy@qcd.lanl.gov

1 INTRODUCTION

The masses of light quarks m_u , m_d , and m_s are three of the least well known parameters of the Standard Model. The range of values listed in the particle data book [1], $2 \leq m_u \leq 8$, $5 \leq m_d \leq 15$, and $100 \leq m_s \leq 300$ (evaluated in the \overline{MS} scheme at $\mu = 1$ GeV), is indicative of the large uncertainty. These quark masses have to be inferred from the masses of low lying hadrons. Theoretically, the best defined procedure is chiral perturbation theory (χ PT) which relates the masses of pseudoscalar mesons to m_u , m_d , and m_s . Recall that the lowest order chiral Lagrangian is

$$\mathcal{L} = \frac{f^2}{8} \text{tr} \left[(\partial_\mu \Sigma \partial_\mu \Sigma^\dagger) + 2\mu(M\Sigma + M\Sigma^\dagger) \right] \quad (1)$$

The presence of the overall unknown scale μ implies that only ratios of quark masses can be determined using χ PT. The predictions from χ PT for the two independent ratios are [2, 3, 4]

	Lowest order	Next order
$2m_s/(m_u + m_d)$	25	24.4(1.5)
m_u/m_d	0.55	0.553(43) .

One notes that the change from lowest to next order is insignificant. Unfortunately, the prospects for further improvement within χ PT are not good. To get absolute numbers, one has to combine the χ PT analysis with sum rule or with some other model calculations. The two most recent and up-to-date versions of the sum rule analysis has been performed by Bijmans, Prades, and de Rafael [5] giving $m_u + m_d = 12(2.5)$ MeV and by Jamin and Munz [6] giving $m_s = 178(18)$ MeV. It is typical of sum rule analysis to quote results at $\mu = 1$ GeV, while lattice results are presented at $\mu = 2$ GeV. To facilitate comparison, we translate the sum-rule values to $\mu = 2$ GeV, whereby $m_u + m_d = 9.4(1.8)$ MeV and $m_s = 126(13)$ MeV using $\Lambda_{\overline{MS}}^{(3)} = 300$ and 380 MeV respectively. These values are about one σ above the quenched lattice results we present below. However, as discussed in [7], a reanalysis of the sum-rules calculations show that the uncertainties are large enough to preclude any serious disagreement with the lattice results. To improve upon the sum-rule estimates requires hard to get at experimental information on the hadronic spectral function. Thus, we believe that lattice QCD offers the best approach to determining these quantities, and this paper presents an analysis of the current data.

In lattice QCD the quark masses are input parameters in the simulations. Their values are determined by tuning the masses of an equal number of hadrons to their physical values. One additional hadron mass is needed to fix the lattice scale, or equivalently the value of α_s . In our lattice simulations we do not include electromagnetic effects, so we can only calculate the isospin symmetric light quark mass $\overline{m} = (m_u + m_d)/2$. The hadrons we use to fix the lattice scale are $M_\rho = 770$ MeV (one could instead, for example, use $f_\pi = 131$ MeV, but its determination is less reliable and has not been reported for all the data we use), while to fix \overline{m} and m_s we study the behavior of pseudoscalar and vector meson masses as a function of the quark mass. (For experimental numbers we use the isospin averaged values $M_\pi = 137$ MeV, $M_K = 495$ MeV, $M_\phi = 1020$ MeV and $M_K^* = 894$ MeV.) We have chosen to use these pseudoscalar and vector mesons since the corresponding correlation functions have been measured with the smallest statistical errors. Thus, in principal, quark masses can be determined without any ambiguity from these calculations.

Current lattice simulations make a number of approximations because of which estimates have systematic errors in addition to statistical errors. Some of these issues have been discussed in the

reviews by Ukawa [8] and Gupta [9]. In this paper we present an analysis of the cumulative world data as available in November 1996 for staggered, Wilson, and Sheikholeslami-Wohlert ($c_{SW} = 1$) fermions, and both for the quenched and $n_f = 2$ theories. (The parameter c_{SW} is the strength of the clover term that is added to the Wilson action to remove the $O(a)$ discretization errors [10, 11].) We present evidence showing that the largest uncertainty in the results arises from discretization ($O(a)$) errors and from the dependence on the number of dynamical flavors. We find that the discretization errors show the expected behavior, $O(a)$ for Wilson and $O(a^2)$ for staggered. For clover action one expects corrections of $O(\alpha_s a)$, however the current data show behavior similar to that with Wilson fermions. By combining the results from these three formulations we show that the discretization errors can be controlled. Thus the main remaining uncertainty is due to extrapolation in n_f , because of which we are only able to extract rough estimates of the quark masses for the physical case of $n_f = 3$. These are significantly smaller than the phenomenological estimates mentioned above, and lead to a large enhancement in the standard model prediction of ϵ'/ϵ .

Lastly, we also present an analysis of the quark condensate, $\langle \bar{\psi}\psi \rangle$, using the data for pseudoscalar meson mass and the Gell-Mann-Oakes-Renner relation. Again we find that the three lattice discretizations of the Dirac action give consistent results after extrapolation to the continuum limit. The condensate turns out to be roughly a factor of two larger than phenomenological estimates such that the renormalization group invariant quantity $m\langle \bar{\psi}\psi \rangle$ is preserved.

This paper is organized as follows. In Section 2 we summarize the definition of the quark mass, the relation between the lattice and continuum results, and the 2-loop running. The reorganization of the lattice perturbation theory *a la* Lepage and Mackenzie is discussed in Section 3. A brief description of the lattice data used in this analysis is given in Section 4. Analyses of \bar{m} and m_s are presented in Sections 5 and 6. We discuss the variation of quark masses with the clover coefficient in Sheikholeslami-Wohlert action in Section 7. A general discussion of the systematic errors is given in Section 8. In Section 9 we compare our results with earlier calculations and discuss the impact on ϵ'/ϵ in Section 10. The calculation of the quark condensate is presented in Sections 11. We end with our conclusions and future outlook in Section 12.

2 DEFINITION OF QUARK MASSES

There are two ways of calculating the \overline{MS} mass for light quarks at scale μ from lattice estimates. The first is

$$\begin{aligned}
m_{\overline{MS}}(\mu) &= Z_m(\mu a)m_L(a) \\
&= \left\{ 1 - \lambda[8\log(\mu a) - C_m] \right\} m_L(a) \\
&\approx \left\{ 1 - \lambda[8\log(\mu a) - (C_m - tad)] \right\} \{m_L(a)X\}
\end{aligned} \tag{2}$$

where $Z_m \equiv 1/Z_S$ is the mass renormalization constant relating the lattice and the continuum regularization schemes at scale μ , and $\lambda = g^2/16\pi^2$. The 1-loop perturbative expressions for Z_m are given in Table 1. For Wilson (or Sheikholeslami-Wohlert (SW) clover) type of fermions, the lattice estimate of the quark mass, defined at scale q^* , is taken to be $m_L(q^*)a = (1/2\kappa - 1/2\kappa_c)$. We have also carried out the analysis using the alternate definition $\text{Ln}(1 + (1/2\kappa - 1/2\kappa_c))$. The change in individual estimates is $\leq 3\%$ for data at $a \lesssim 0.5 \text{ GeV}^{-1}$ and negligible in the extrapolated values. Since the analysis with this $O(a)$ improved definition is much less transparent we use the simpler

form. For staggered fermions $m_L(q^*) = m_0$, the input mass. The last form in Eq. 2 shows the result of applying tadpole improvement as discussed in Section 3.

The second method is to use the Ward Identity for the renormalized axial vector current, $\partial_\mu Z_A A_\mu = (m_1 + m_2) Z_P P + O(a)$, where m_1 and m_2 are the masses of the two fields in the bilinear operators. The quark mass, to $O(a)$, is then given by the following ratio of correlation functions

$$(m_1 + m_2) = \frac{Z_A \langle \partial_4 A_4(\tau) J(0) \rangle}{Z_P \langle P(\tau) J(0) \rangle}. \quad (3)$$

where $J(0)$ is any interpolating field operator that produces pions at $\vec{p} = 0$. Here, Z_A and Z_P are the renormalization constants for the axial and pseudoscalar densities that match the lattice and continuum theories at scale $\mu = q^*$. The important point to note is that since the Ward identity is valid locally, the value of m should be independent of τ . Violations of this relation are signals for $O(a)$ errors in the currents. This has been exploited by the Alpha collaboration to remove the $O(a)$ discretization errors non-perturbatively in the clover action and currents [11].

At long time separation (τ large) one can assume that the 2-point correlation function is described by the asymptotic form $\sim e^{-m\pi\tau}$. One can then write Eq. 3 as

$$(m_1 + m_2) = \frac{Z_A}{Z_P} m_\pi \frac{\langle A_4(\tau) J(0) \rangle}{\langle P(\tau) J(0) \rangle}. \quad (4)$$

There are very few calculations of m_q using these two versions of the Ward Identity. Also, at this stage the perturbative and non-perturbative estimate of Z_P do not agree [12]. For these reasons we postpone the discussion of this method to a later work [13].

Once $m_{\overline{MS}}$ has been calculated at the continuum scale μ , its value at any other scale Q is given by the two loop running [12]

$$\frac{m(Q)}{m(\mu)} = \left(\frac{g^2(Q)}{g^2(\mu)} \right)^{\gamma_0/2\beta_0} \left(1 + \frac{g^2(Q) - g^2(\mu)}{16\pi^2} \left(\frac{\gamma_1\beta_0 - \gamma_0\beta_1}{2\beta_0^2} \right) \right). \quad (5)$$

where in the \overline{MS} scheme for N colors and n_f flavors

$$\begin{aligned} \beta_0 &= \frac{11N - 2n_f}{3}, \\ \beta_1 &= \frac{34}{3}N^2 - \frac{10}{3}Nn_f - \frac{N^2 - 1}{N}n_f, \\ \gamma_0 &= 6\frac{N^2 - 1}{2N}, \\ \gamma_1 &= \frac{97N}{3}\frac{N^2 - 1}{2N} + 3\left(\frac{N^2 - 1}{2N}\right)^2 - \frac{10n_f}{3}\frac{N^2 - 1}{2N}. \end{aligned} \quad (6)$$

We will quote our final numbers at $Q = 2$ GeV as we do not feel confident using the 2-loop relations to run to smaller scales.

3 Renormalization Constants

Our final results are stated in the \overline{MS} scheme. The required 1-loop renormalization constants for matching the lattice and continuum operators for Wilson, clover, and staggered versions of the lattice discretization are collected in Table 1 using results derived in [14, 15, 16]. We reorganize

Table 1: Renormalization constants in the \overline{MS} scheme before tadpole subtraction for staggered [15], and Wilson and clover ($c_{SW} = 1$) [16] fermions. Here $\lambda = g^2/16\pi^2$.

	<i>Staggered</i>	<i>Wilson</i>	<i>Clover</i> ($c_{SW} = 1$)
Z_A	1	$1 - 21.06\lambda$	$1 - 18.39\lambda$
Z_P	$1/Z_m$	$1 + \lambda(8\ln(\mu a) - 30.13)$	$1 + \lambda(8\ln(\mu a) - 29.84)$
Z_m	$1 - \lambda(8\ln(\mu a) - 52.288)$	$1 - \lambda(8\ln(\mu a) - 17.27)$	$1 - \lambda(8\ln(\mu a) - 25.75)$

lattice perturbation theory using the Lepage-Mackenzie prescription [17]. This prescription involves four parts: the renormalization of the quark field Z_ψ and the quark mass, the removal of tadpole contribution from the 1-loop operator renormalization, the choice of α_s , and an estimate of the typical scale q^* characterizing the lattice calculation.

We use the following Lepage-Mackenzie definition of the strong coupling constant [17, 18, 19],

$$\begin{aligned}
 -\ln\langle\frac{1}{3}\text{Tr}plaq\rangle &= \frac{4\pi}{3}\alpha_V(3.41/a) (1 - (1.191 + 0.025n_f)\alpha_V) && (Wilson), \\
 &= \frac{4\pi}{3}\alpha_V(3.41/a) (1 - (1.191 + 0.070n_f)\alpha_V) && (Stag.), \tag{7}
 \end{aligned}$$

from which the \overline{MS} coupling at scale $3.41/a$ is given by

$$\alpha_{\overline{MS}}(3.41/a) = \alpha_V(e^{5/6}3.41/a)(1 + \frac{2}{\pi}\alpha_V). \tag{8}$$

The value of $\alpha_{\overline{MS}}$ at any other scale is then obtained by integrating the standard 2-loop β -function for the appropriate number of flavors. The results are given in Tables 2, 3, and 6. Ideally, $\alpha_{\overline{MS}}(2 \text{ GeV})$ should be independent of β . From these tables one can see the variation with β , and the extent to which the variation in $1/a$ at fixed β feeds into $\alpha_{\overline{MS}}(2 \text{ GeV})$. Reorganizing the lattice perturbation theory in terms of $\alpha_{\overline{MS}}$ has the advantage that the continuum and lattice α_s is the same when matching the theories at scale $\mu = q^*$. We call this matching procedure ‘‘horizontal’’ matching [20].

An estimate of q^* is not straightforward since Z_m is logarithmically divergent. So we appeal to the general philosophy of tadpole improvement, *i.e.* it is designed to remove the short-distance lattice artifacts. Once these have been removed, the typical scale q^* of the lattice calculation becomes less ultraviolet. Thus, our preferred scheme is one in which $q^* = \mu = 1/a$, which we call *TAD1*. To analyze the dependence of the results on q^* we also investigate the choices $q^* = \mu = 0.5/a, 2/a$ and π/a . A more detailed description of these schemes and our implementation of the matching between the lattice and continuum is given in [20].

In all methods of calculating the quark mass, Eqs. 2, 3, 4, the normalization of the quark fields does not enter, or cancels between the different currents. Thus, one does not have to consider this factor. The quark mass gets scaled by the tadpole factor X , *i.e.* $m_L \rightarrow Xm_L$, where we use the non-perturbatively determined estimate for X .

The tadpole factor X for Wilson and clover fermions is chosen to be $8\kappa_c$ [21]. It has the perturbative expansion $X = 1 + tad \lambda$ where

$$\begin{aligned}
 tad &= 17.14, && (Wilson), \\
 tad &= 10.66, && (Clover (c_{SW} = 1)). \tag{9}
 \end{aligned}$$

For Wilson fermions at, say, $\beta = 6.0$, $\lambda = 0.0153$ in the *TAD1* prescription, so the perturbative value $8\kappa_c = 1.262$ is almost identical to our non-perturbative estimate $8\kappa_c = 1.257$ [22]. The

Lepage-Mackenzie reorganization, as shown in Eq. 2, therefore seems benign, nevertheless, we include tadpole subtraction as its purpose, in general, is to reorganize lattice perturbation theory to make the neglected higher order corrections small. The entries in Table 1 show that after tadpole subtraction the 1-loop corrections are indeed smaller for Wilson and clover fermions. However, note that the 1-loop results presented in [16], and used here, show that the perturbative correction grows with c_{SW} .

For staggered fermions we define the tadpole factor X as the inverse of the fourth root of the expectation value of the plaquette

$$X = U_0^{-1} = \text{plaquette}^{-1/4} = (1 + 13.16\lambda) . \quad (10)$$

The agreement, at $\beta = 6.0$, between the perturbative value 1.20 and the non-perturbative value 1.14 is still reasonable in *TAD1*, even though the plaquette is designed to match at $q^* \approx 3.41/a$ as shown in Eq. 7. The point to note is that for any reasonable choice of X , the correction $C_m - \text{tad}$ is still very large for staggered fermions. Thus one might doubt whether the 1-loop perturbative result for Z_m is reliable. It turns out, as we show later, that using the expressions given in Table 1 give results that, in the $a \rightarrow 0$ limit, agree with those obtained using Wilson-like fermions.

The second noteworthy outcome of our analysis is that the dependence of the results on the choice of q^* , and whether or not one does tadpole subtraction, are small. We find that m increases with q^* , and the most significant variation is in the quenched staggered data ($\sim 5\%$). The difference between tadpole subtraction and no tadpole subtraction is significant only at strong coupling ($\sim 3\%$ at $\beta = 6.0$ for the quenched theory, and $< 3\%$ for $\beta \geq 5.4$ for $n_f = 2$), and even smaller for different choices of tadpole factor. Based on the above estimates we assume that for $a \lesssim 0.5$ the uncertainty in relating the lattice results to those in a continuum scheme is under control at the 5% level. We consider this variation negligible since for many of the data points it is small compared to even the statistical errors. Furthermore, this uncertainty is one aspect of the discretization errors, and our estimate of the errors associated with the extrapolation to $a \rightarrow 0$ incorporates it. To summarize, all of our lattice estimates are quoted using the *TAD1* scheme, and the uncertainty associated with this choice is included in our quoted extrapolation error.

4 LATTICE PARAMETERS OF DATA ANALYZED

The list of calculations from which we have taken data are summarized in Tables 2 and 3. The quenched Wilson data are taken from Refs. [18, 22, 23, 24, 25, 26, 27, 28], quenched staggered from [19, 29, 30, 31, 32, 33], quenched clover from [27], dynamical ($n_f = 2$) Wilson from [34, 35, 36, 37], and dynamical ($n_f = 2$) staggered fermions from [19, 38, 39]. All these calculations use the simple Wilson (plaquette) action for the gauge fields. Thus the difference between staggered and Wilson-like fermion data for fixed n_f is a reflection of the difference in $O(a)$ errors between the various discretization schemes.

In principle, if lattice simulations could be done with three dynamical flavors and with realistic parameters, one could tune the three quark masses to reproduce the spectrum and thereby determine their values. However, since this is not the case, the strategy we use is as follows. For each value of the lattice parameters (β , n_f , fermion action) we fit the data for M_π^2 and M_ρ as a linear function of the quark mass

$$\begin{aligned} M_\pi^2 &= A_\pi + B_\pi(m_1 + m_2)/2 \\ M_\rho &= A_\rho + B_\rho(m_1 + m_2)/2 , \end{aligned} \quad (11)$$

Table 2: Lattice parameters of the quenched data used in the global analysis. We list the reference, the type of fermion action (W =Wilson, S =staggered, C =clover with $c_{SW} = 1$), the coupling $\beta = 6/g^2$, the lattice size, the number of configurations in the statistical sample, the values of quark masses in lattice units (κ values) used in the fits for staggered (Wilson and clover) fermions, the lattice scale $1/a$ GeV extracted from M_ρ , and the values of $\alpha_{\overline{MS}}$ at $q^* = 1/a$ and 2 GeV.

Label	Ref.	β	Lattice size	# of Conf.	Quark masses used in the fits	Scale $1/a$ (GeV)	$\alpha_{\overline{MS}}(q^*)$ (1/a) (2 GeV)
W1	[23]	5.7	$24^3 \times 32$	50	0.165, 0.167, 0.168	1.431(27)	0.246 0.211
W2	[25]	5.7	$24^3 \times 32$	92	0.165, 0.1663, 0.1675	1.422(24)	0.246 0.210
W3	[26]	5.85	$24^3 \times 54$	100	0.1585, 0.1595, 0.1605	1.958(114)	0.213 0.211
W4	[18]	5.85	$16^3 \times 32$	90	0.1585, 0.1600	1.741(76)	0.213 0.201
W5	[24]	5.9	$16^3 \times 40$	150	0.156, 0.157, 0.158, 0.1585	1.987(48)	0.205 0.204
W6	[25]	5.93	$24^3 \times 36$	210	0.156, 0.1573, 0.1581	2.000(37)	0.201 0.201
W7	[18]	5.95	$16^3 \times 32$	90	0.1554, 0.1567	1.941(58)	0.198 0.196
W8	[22]	6.0	$32^3 \times 64$	170	0.155, 0.1558, 0.1563	2.338(43)	0.192 0.205
W9	[23]	6.0	$24^3 \times 32$	78	0.155, 0.1558, 0.1563	2.204(70)	0.192 0.200
W10	[26]	6.0	$24^3 \times 54$	200	0.155, 0.1555, 0.1563	2.423(146)	0.192 0.208
W11	[27]	6.0	$18^3 \times 64$	320	0.153, 0.154, 0.155	2.154(64)	0.192 0.198
W12	[24]	6.1	$24^3 \times 64$	100	0.152, 0.153, 0.154, 0.1543	2.629(59)	0.181 0.201
W13	[25]	6.17	$32^3 \times 40$	219	0.1519, 0.1526, 0.1532	2.755(48)	0.176 0.198
W14	[28]	6.2	$24^3 \times 48$	18	0.1523, 0.1526, 0.1529	2.735(172)	0.173 0.194
W15	[27]	6.2	$24^3 \times 64$	250	0.1510, 0.1515, 0.1520, 0.1526	2.914(89)	0.173 0.199
W16	[27]	6.2	$24^3 \times 64$	110	0.1510, 0.1520, 0.1526	2.934(121)	0.173 0.200
W17	[24]	6.3	$32^3 \times 80$	100	0.150, 0.1505, 0.151, 0.1513	3.260(88)	0.166 0.197
W18	[23]	6.3	$24^3 \times 32$	128	0.1485, 0.1498, 0.1505	3.092(68)	0.166 0.193
W19	[23]	6.4	$24^3 \times 60$	15	0.1485, 0.1490, 0.1495	3.628(416)	0.159 0.195
W20	[27]	6.4	$24^3 \times 64$	400	0.1488, 0.1492, 0.1496, 0.1500	4.095(163)	0.159 0.205
S1	[29]	5.7	$24^3 \times 32$	50	0.02, 0.015, 0.01, 0.005		
	[31]	5.7	$16^3 \times 32$	32	0.02, 0.015, 0.01, 0.005	0.951(78)	0.246 0.180
S2	[19]	5.85	$16^3 \times 32$	160	0.025, 0.01	1.312(75)	0.213 0.180
S3	[30]	5.85	$16^3 \times 32$	60	0.01, 0.02, 0.03, 0.04	1.340(31)	0.213 0.182
S4	[30]	5.93	$20^3 \times 40$	50	0.01, 0.02, 0.03, 0.04	1.571(33)	0.201 0.183
S5	[19]	5.95	$16^3 \times 32$	190	0.025, 0.01	1.645(25)	0.198 0.184
S6	[29]	6.0	$24^3 \times 32$	60	0.04, 0.02, 0.01	1.843(78)	0.192 0.187
S7	[31]	6.0	$24^3 \times 40$	23	0.03, 0.025, 0.02, 0.015, 0.01	1.911(84)	0.192 0.189
S8	[32]	6.0	$32^3 \times 64$	200	0.01, 0.005, 0.0025	1.917(34)	0.192 0.189
S9	[30]	6.0	$24^3 \times 64$	50	0.02, 0.03, 0.04	1.855(41)	0.192 0.187
S10	[31]	6.2	$32^3 \times 48$	23	0.025, 0.015, 0.01, 0.005	2.569(78)	0.173 0.189
S11	[30]	6.2	$32^3 \times 64$	40	0.005, 0.01, 0.02	2.616(91)	0.173 0.191
S12	[31]	6.4	$32^3 \times 48$	24	0.015, 0.010, 0.005	3.467(376)	0.159 0.192
S13	[30]	6.4	$40^3 \times 96$	40	0.005, 0.01, 0.02	3.429(78)	0.159 0.191
S14	[32]	6.5	$32^3 \times 64$	100	0.01, 0.005, 0.0025	3.962(127)	0.152 0.192
S15	[33]	6.5	$48^3 \times 64$	200	0.01, 0.005, 0.0025	3.811(59)	0.152 0.189
C1	[27]	6.0	$18^3 \times 64$	200	0.1425, 0.1432, 0.1440	1.867(81)	0.192 0.187
C2	[27]	6.2	$24^3 \times 64$	250	0.14144, 0.14184, 0.14224, 0.14264	2.604(131)	0.173 0.190
C3	[27]	6.2	$18^3 \times 64$	200	0.14144, 0.14190, 0.14244	3.082(384)	0.173 0.204
C4	[27]	6.4	$24^3 \times 64$	400	0.1400, 0.1403, 0.1406, 0.1409	3.951(182)	0.159 0.202

Table 3: Lattice parameters of the $n_f = 2$ dynamical simulation data we use in the global analysis. The rest is same as in Table 2.

Label	Ref.	β	Lattice size	# of Conf.	Quark masses used in the fits	Scale $1/a$ (GeV)	$\alpha_{\overline{MS}}(q^*)$ ($1/a$)	$\alpha_{\overline{MS}}(q^*)$ (2 GeV)
\mathcal{W}_21	[36]	5.3	$16^3 \times 32$	417-484	0.167, 0.1675	1.890(110)	0.266	0.259
\mathcal{W}_22	[34]	5.4	$16^3 \times 32$	14-15	0.160, 0.161, 0.162	1.467(113)	0.254	0.223
\mathcal{W}_23	[34]	5.5	$16^3 \times 32$	15-27	0.158, 0.159, 0.160	1.812(97)	0.227	0.219
\mathcal{W}_24	[36]	5.5	$16^3 \times 32$	400-669	0.1596, 0.1600, 0.1604	2.179(84)	0.226	0.234
\mathcal{W}_25	[34]	5.6	$16^3 \times 32$	32-45	0.156, 0.157	2.332(209)	0.213	0.226
\mathcal{W}_26	[37]	5.6	$16^3 \times 32$	100	0.156, 0.157, 0.1575	2.379(77)	0.213	0.227
\mathcal{S}_21	[19]	5.6	$16^3 \times 32$	200-400	0.025, 0.01	1.798(73)	0.232	0.223
\mathcal{S}_22	[39]	5.7	$16^3 \times 32$	~ 50	0.025, 0.02, 0.015, 0.01	2.341(78)	0.216	0.230
\mathcal{S}_23	[38]	5.7	$20^3 \times 20$	150-160	0.02, 0.01	2.236(99)	0.216	0.226

where m_1 and m_2 are the masses of the two quarks. (We use M_π as shorthand for pseudoscalars, and M_ρ for vector mesons.) These fits are made assuming that the data at each value of the quark mass are independent, and the statistical error estimates quoted by the authors are used in the χ^2 minimization procedure. Note that for Wilson-like fermions we make fits to $1/2\kappa$ whereby A_π defines κ_c and A_ρ is the intercept at $1/2\kappa = 0$. For staggered fermions A_π should be zero due to chiral symmetry. However, in our analysis we leave it as a free parameter and use it to define the zero of the quark mass. This leaves B_π, A_ρ, B_ρ from which we determine the three quantities that we are interested in; the scale using M_ρ , \overline{m} using M_π^2/M_ρ^2 , and m_s in three different ways using M_K, M_{K^*}, M_ϕ . Throughout the analysis we assume that ϕ is a pure $s\bar{s}$ state.

The error analysis of the global data is somewhat limited since in most cases we only have access to the final published numbers. For this reason we cannot include two types of correlations in the data when making fits using Eq. 11. Firstly, those between pseudoscalar and vector mesons at a given quark mass, and secondly those between the meson masses at different quark masses calculated on the same background gauge configurations as is the case for the quenched simulations. Thus, when making chiral fits we simply assume that the errors in the lattice measurements of meson masses are uncorrelated. Thereafter, the errors in $A_\pi, B_\pi, A_\rho, B_\rho$ are propagated self-consistently to the final estimates. By comparing results in a few cases where a full error analysis has been done, we find that these shortcomings change estimates of individual points by less than even the statistical errors. The one exception is the results from QCDPAX collaboration [26] where the neglected correlations have a large effect. They quote significantly different values for $A_\pi, B_\pi, A_\rho, B_\rho$ based on correlated fits. Using their correlated fit parameters give quark masses consistent with other estimates at the same couplings. Thus, we believe that our estimates based on a reanalysis of the global data are reliable.

The input parameters and results ($\alpha_{\overline{MS}}$, lattice scale $1/a$, $A_\pi, B_\pi, A_\rho, B_\rho$, and the quark masses in lattice units and in MeV in \overline{MS} scheme at 2 GeV) for each data set are given in Tables 2, 3, 6, 4, 5, and 7. (In the case of data from Ref. [30], the analysis started with the results for $A_\pi, B_\pi, A_\rho, B_\rho$ because the raw data have not been published.) We note that the various data points are obtained on lattices of different physical volumes, the statistical sample size varies significantly (the sample size is rather small in some cases), and the strategy for extracting masses varies from group to group. However, it turns out that in the calculation of quark masses, there is a cancellation of errors that make these differences much less significant than for example in the estimates of meson masses themselves. We substantiate some of these remarks by presenting a detailed analysis of

some of the systematic errors in Section 8 using data from our high statistics calculation presented in Ref. [22].

Once we have the quark masses at different lattice scales, we analyze the dependence on the lattice spacing a by comparing Wilson, clover, and staggered results. Where data permit, we omit points at the stronger couplings (larger a) for the following two reasons. First, we use only the leading correction in the extrapolation to $a = 0$, and secondly, the perturbative matching becomes less reliable as β is decreased. The end result is that we find that the leading corrections give a good fit to the data, and in the $a = 0$ limit the different fermion formulations give consistent results.

To investigate the n_f dependence, we compare the $n_f = 0$ and $n_f = 2$ results. We then assume a linear behavior in n_f to extrapolate these two points to estimate the desired physical value. As we make clear in our discussions, the extrapolation in n_f turns out to be the weakest part of our analysis.

5 LIGHT QUARK MASS $\overline{m} = (m_u + m_d)/2$

In order to extract light quark masses from lattice simulations we have used the simplest ansatz, Eq. 11, for the chiral behavior of hadron masses. The reason for this truncation is that in most cases the data for M_π and M_ρ exist at only 2 – 4 values of “light” quark masses in the range $0.3m_s - 2m_s$. In this restricted range of quark masses the existing data do not show any significant deviation from linearity. Using linear fits to M_π^2 data over a limited range in m_q means that we can predict only one independent quark mass from the pseudoscalar data, and we cannot test the difference between tree level and NLO results predicted by χ PT analyses. The mass we prefer to extract using the pseudoscalar spectrum, barring the complications of quenched χ PT which are expected to become significant only for $m_q \lesssim 0.3m_s$ [9, 40], is \overline{m} because to extract m_s using m_K needs first an extrapolation to \overline{m} in the light quark. While this choice avoids the question whether lowest order χ PT is valid up to m_s , one must bear in mind that the fits are made to data in the “heavier” range $0.3m_s \leq m_q \sim 2m_s$ and then extrapolated to \overline{m} . The bottom line is that to get \overline{m} we linearly extrapolate the ratio M_π^2/M_ρ^2 in m to its physical value 0.03166.

The global quenched data are shown in Fig. 1 and listed in Table 4 for the tadpole subtraction scheme TAD1. The expected leading term in the discretization errors is $O(a)$ for Wilson, $O(g^2a)$ for clover, and $O(a^2)$ for staggered. The fits, keeping only the leading dependence (for clover data we assume a linear dependence in a), give

$$\begin{array}{lll} m(a) = 3.33(22) \text{ MeV } [1 + 1.3(2) \text{ GeV } a] & \chi^2/dof = 0.8 & \text{Wilson} \\ m(a) = 3.13(42) \text{ MeV } [1 + 1.4(4) \text{ GeV } a] & \chi^2/dof = 0.6 & \text{Clover} \\ m(a) = 3.27(04) \text{ MeV } [1 + (0.20(11) \text{ GeV } a)^2] & \chi^2/dof = 4.6 & \text{Staggered} . \end{array}$$

For Wilson and staggered fermions we fit to $\beta \geq 5.93$ ($a \lesssim 0.5 \text{ GeV}^{-1}$) to minimize the effect of higher order corrections. The staggered data show a small rise for $\beta \geq 6.0$ after the initial fall. With present data it is not clear whether this is due to poor statistics, the decreasing physical volume of the lattices used, or higher order terms in a and g^2 . As a result, the fit with only the lowest order correction is not able to capture this trend in the data. This is reflected in the high χ^2/dof . Thus we consider, as an alternate estimate of the continuum result, the mean, $\overline{m} = 3.4(1) \text{ MeV}$, of the estimates at the two highest β . A second alternative is to fit the data for $\beta \geq 6.0$. This give $\overline{m} = 3.53(6) \text{ MeV}$ with a $\chi^2/dof = 0.95$. The corresponding fit for Wilson fermions gives $\overline{m} = 3.45(23) \text{ MeV}$ with a $\chi^2/dof = 0.9$.

Given the size of $O(a)$ corrections in the case of Wilson fermions, we have also fit the data including a quadratic correction as shown in Fig. 2. Unfortunately, we find that even the sign of

Table 4: Results for the fit parameters κ_c for Wilson-like and A_π for staggered fermions, B_π , A_ρ and B_ρ , defined in Eq. 11, and the quark masses for the quenched simulations. Both the lattice values, $\bar{m}a$ and $m_s(M_\phi)a$, as well as the physical values, $\bar{m}(\overline{MS}, 2 \text{ GeV})$ and $m_s(\overline{MS}, 2 \text{ GeV}, M_\phi)$ in MeV, are given. The lattice parameters and the references to the original work are given in Table 2. Chiral fits for labels marked by a * have $\chi^2/dof \geq 3.0$.

Label	κ_c/A_π	B_π	A_ρ	B_ρ	\bar{m}		$m_s(M_\phi)$	
					$\bar{m}a \times 10^5$	\bar{m}	$m_s a \times 10^3$	m_s
W1	0.169250(11)	2.758(43)	-4.221(481)	1.609(160)	332(13)	6.05(14)	112(13)	204(20)
W2	0.169308(12)	2.712(38)	-4.223(422)	1.612(140)	342(12)	6.19(13)	113(11)	203(17)
W3	0.161605(02)	2.334(33)	-6.840(1372)	2.336(436)	210(24)	5.30(31)	57(14)	143(26)
W4	0.161662(17)	2.317(75)	-4.161(1150)	1.487(366)	267(24)	5.89(30)	99(28)	219(53)
W5	0.159811(11)	2.309(39)	-5.819(471)	1.982(148)	206(10)	5.24(14)	66(06)	167(12)
W6	0.158950(06)	2.141(32)	-5.086(473)	1.738(148)	219(08)	5.59(13)	74(07)	189(16)
W7	0.158379(13)	2.166(49)	-4.453(701)	1.535(218)	230(14)	5.64(20)	86(14)	211(29)
W8	0.157143(03)	1.993(26)	-6.663(521)	2.196(162)	172(06)	5.20(11)	50(05)	152(11)
W9	0.157122(08)	2.037(60)	-5.680(993)	1.894(309)	190(13)	5.35(22)	62(12)	174(28)
W10	0.157135(05)	2.005(50)	-7.556(1561)	2.473(485)	159(19)	5.02(32)	43(11)	136(26)
W11	0.157024(06)	2.130(24)	-5.494(477)	1.837(146)	190(11)	5.21(16)	65(07)	179(14)
W12	0.154978(03)	1.862(20)	-6.537(400)	2.116(122)	146(07)	4.97(12)	46(04)	158(9)
W13	0.153760(04)	1.740(31)	-6.365(477)	2.042(145)	142(05)	5.06(11)	46(04)	163(11)
W14	0.153308(14)	1.746(104)	-6.128(1603)	1.964(487)	144(19)	5.06(41)	48(14)	169(41)
W15	0.153292(02)	1.678(17)	-6.632(604)	2.113(183)	132(08)	4.99(16)	42(05)	159(13)
W16	0.153292(03)	1.708(24)	-7.021(793)	2.232(240)	128(11)	4.87(21)	39(06)	151(16)
W17	0.151796(02)	1.546(22)	-6.832(631)	2.145(190)	114(06)	4.86(14)	37(04)	157(14)
W18	0.151637(15)	1.734(31)	-6.968(290)	2.188(86)	113(05)	4.53(10)	38(02)	152(6)
W19	0.150632(132)	1.517(236)	-7.511(1686)	2.326(502)	94(18)	4.47(58)	31(09)	145(31)
W20	0.150580(05)	1.385(31)	-8.435(696)	2.596(208)	81(06)	4.42(18)	24(03)	133(10)
S1*	-0.0005429(05)	7.806(33)	0.791(71)	8.879(4405)	266(43)	4.56(37)	32(17)	54(26)
S2	-0.0007702(79)	6.986(49)	0.583(34)	5.333(1392)	156(18)	3.66(21)	37(12)	86(22)
S3		6.700(20)	0.567(13)	4.960(280)	156(07)	3.74(09)	39(02)	94(5)
S4		6.150(10)	0.484(10)	4.840(200)	124(05)	3.48(07)	34(02)	96(4)
S5	-0.0007099(174)	5.840(47)	0.466(07)	5.133(377)	119(04)	3.50(06)	30(03)	89(7)
S6	-0.0002067(154)	5.634(45)	0.414(18)	5.323(588)	98(08)	3.25(14)	26(04)	87(10)
S7	-0.0000768(174)	5.666(65)	0.398(18)	5.736(786)	91(08)	3.14(14)	24(04)	82(11)
S8*	-0.0001874(03)	5.690(20)	0.396(08)	7.717(1197)	90(03)	3.11(06)	18(03)	61(9)
S9		5.610(10)	0.410(09)	5.140(170)	97(04)	3.25(07)	27(01)	91(3)
S10*	-0.0000717(57)	4.020(29)	0.297(09)	5.019(484)	71(04)	3.28(10)	20(02)	93(9)
S11		4.010(20)	0.291(10)	4.880(400)	68(05)	3.24(11)	20(02)	96(8)
S12	0.0000310(239)	2.884(110)	0.219(24)	4.851(1850)	54(12)	3.39(38)	15(07)	97(36)
S13		2.970(20)	0.222(05)	4.760(200)	54(02)	3.33(08)	16(01)	98(4)
S14	-0.0001986(107)	2.482(56)	0.193(06)	4.880(723)	48(03)	3.45(13)	13(02)	95(14)
S15*	0.0001403(24)	2.518(18)	0.199(03)	3.937(365)	51(02)	3.52(06)	17(02)	119(11)
C1	0.145483(03)	2.674(29)	-6.265(1006)	1.942(288)	201(18)	5.33(24)	71(13)	188(27)
C2	0.143150(02)	2.076(27)	-7.378(1373)	2.196(389)	133(13)	4.99(26)	45(10)	169(29)
C3	0.143100(08)	2.110(93)	-10.897(2879)	3.189(815)	94(23)	4.26(54)	26(10)	120(30)
C4	0.141439(04)	1.695(40)	-10.849(949)	3.123(266)	71(06)	4.16(19)	21(03)	123(10)

Table 5: The results for the $n_f = 2$ dynamical simulations listed in Table 3. The notation is same as in Table 4.

Label	κ_c/A_π	B_π	A_ρ	B_ρ	\overline{m}		$m_s(M_\phi)$	
					$\overline{m}a \times 10^5$	\overline{m}	$m_s a \times 10^3$	m_s
\mathcal{W}_21	0.167928(07)	12.471(365)	-41.186(4356)	13.967(1455)	42(05)	1.06(06)	10(02)	25(3)
\mathcal{W}_22	0.164866(288)	6.287(440)	-10.566(1450)	3.655(466)	139(20)	2.53(20)	48(09)	88(11)
\mathcal{W}_23	0.161335(64)	4.979(225)	-11.542(1239)	3.860(393)	115(11)	2.64(15)	37(06)	85(9)
\mathcal{W}_24	0.161218(08)	4.499(134)	-14.173(1801)	4.683(576)	88(07)	2.52(11)	25(04)	73(9)
\mathcal{W}_25	0.158393(47)	4.426(285)	-14.249(2216)	4.617(694)	78(13)	2.37(21)	24(06)	73(11)
\mathcal{W}_26^*	0.158506(13)	3.903(87)	-13.211(823)	4.290(258)	85(05)	2.65(09)	25(02)	79(5)
\mathcal{S}_21^*	-0.00025(1)	6.951(66)	0.423(17)	8.667(777)	84(07)	2.93(12)	17(02)	58(5)
\mathcal{S}_22	0.00012(7)	6.041(98)	0.323(11)	9.120(501)	57(04)	2.62(09)	12(01)	57(3)
\mathcal{S}_23	-0.00078(11)	5.573(162)	0.345(14)	7.320(762)	67(06)	2.95(14)	15(02)	66(8)

the quadratic term changes depending on whether we include all the points with $\beta \geq 5.93$ or only those with $\beta \geq 6.0$. Also, one cannot distinguish between the three fits on the basis of χ^2/dof which lies between 0.8 – 0.96. The lack of stability of the quadratic fits indicates that possible $O(a^2)$ corrections cannot be determined with the current data. For this reason we use the results obtained using the lowest order fit as our best estimate.

The clover ($c_{SW} = 1$) fermion results are surprisingly close to the Wilson values even though the discretization errors should be smaller, *i.e.* $O(g^2 a)$. In particular the variation with β is similar to that for Wilson fermions, however it should be noted that this is based on data at only three values of β . At present, looking at the trend in the data, the best we can do is to assume a linear behavior.

The bottom line is that the results, in the $a = 0$ limit, from all three formulations turn out to be in surprisingly good agreement with each other. Thus, for our best estimate of the quenched value we take an average of the $\beta \geq 6.0$ numbers

$$\overline{m}(\overline{MS}, 2 \text{ GeV}) = 3.4 \pm 0.4 \pm 0.3 \text{ MeV} \quad (\text{quenched}). \quad (12)$$

where the first error estimate is the largest of the extrapolation errors and covers the spread in the data. The second error is a 10% uncertainty due to the lattice scale as discussed in Section 8.

To analyze the $n_f = 2$ dynamical configurations, we have restricted ourselves to data with $m_{valence} = m_{sea}$. The main limitation we face is that the data have been obtained at very few values of lattice spacing, and the statistics and lattice volumes are smaller than in quenched simulations. The pattern of $O(a)$ corrections in the present unquenched data, shown in Fig. 3 and Table 5, is not clear. In fact, as discussed in Section 8, we cannot even ascertain whether the convergence in a is analogous to the quenched case, *i.e.* from above for both Wilson and staggered formulations. The strongest statement we can make is qualitative; at any given value of the lattice spacing, the $n_f = 2$ data lies below the quenched result. Taking the existing data at face value, we find that the average of the Wilson and staggered values are the same for the choices $\beta \geq 5.4$, $\beta \geq 5.5$, or $\beta \geq 5.6$. Since for $\beta \geq 5.5$ there are two independent measurements that agree, our current estimate is taken to be the average of these data

$$\overline{m}(2 \text{ GeV}) = 2.7 \pm 0.3 \pm 0.3 \text{ MeV} \quad (n_f = 2 \text{ flavors}), \quad (13)$$

where the first error estimate is the spread in the data. To obtain a value for the physical case of $n_f = 3$, the best we can do is to assume a behavior linear in n_f . In this case a linear extrapolation of the $n_f = 0$ and 2 data gives

$$\overline{m}(2 \text{ GeV}) \approx 2.4 \text{ MeV} \quad (n_f = 3 \text{ flavors}). \quad (14)$$

It is obvious that more lattice data are needed to resolve the behavior of the unquenched results. However, the surprise of this analysis is that both the quenched and $n_f = 2$ values are small and lie at the very bottom of the range predicted by phenomenological analyses [2].

6 THE STRANGE QUARK MASS m_s

We determine m_s using the three different mass-ratios, M_K^2/M_π^2 , M_{K^*}/M_ρ , and M_ϕ/M_ρ . As mentioned above, using a linear fit to the pseudo-scalar data constrains $m_s(M_K)/\overline{m} = 25.9$. Unfortunately, the data are not good enough to include terms of order m_q^2 or the non-analytical chiral logarithms when making fits. Thus we cannot improve on the lowest order results

$$\begin{aligned} m_s(\overline{MS}, \mu = 2 \text{ GeV}, M_K) &= 88(10) \text{ MeV} && \text{(Quenched)}, \\ m_s(\overline{MS}, \mu = 2 \text{ GeV}, M_K) &= 70(8) \text{ MeV} && (n_f = 2), \end{aligned} \quad (15)$$

when extracting m_s from M_K^2/M_π^2 . Using the vector mesons M_K^* and M_ϕ gives independent estimates. To illustrate the difference, a comparison of $m_s(M_\phi)$ and $m_s = 25.9\overline{m}$ is shown in Fig. 4 for the quenched Wilson theory.

The quenched Wilson and staggered data, and the extrapolation to $a = 0$, for $m_s(M_\phi)$ are shown in Fig. 5. The Wilson data again show large $O(a)$ corrections and we make a linear fit to the data at $\beta \geq 5.93$. The staggered data converges from below, and anticipating $O(a^2)$ corrections we fit linearly in a^2 . The clover data are shown in Fig. 6. The parameters of the fits are

$$\begin{aligned} m_s(M_\phi) &= 94(18) \text{ MeV}[1 + 1.9(7) \text{ GeV } a] && \chi^2/dof = 0.4 && \text{Wilson} \\ m_s(M_\phi) &= 62(31) \text{ MeV}[1 + 3.9(2.5) \text{ GeV } a] && \chi^2/dof = 0.34 && \text{Clover} \\ m_s(M_\phi) &= 99(4) \text{ MeV}[1 - (0.48(15) \text{ GeV } a)^2] && \chi^2/dof = 2.0 && \text{Staggered} . \end{aligned} \quad (16)$$

Compared to \overline{m} , Wilson and clover fits have much larger errors. This is due to the fact that the lattice measurements of the vector mass have much larger statistical errors compared to the pseudoscalars. Also, the spread between different groups is larger, reflecting the differences in the strategy to extract the masses from the 2-point correlation functions. The fit to the staggered data for m_s , on the other hand, is surprisingly much better than that for \overline{m} . Since the parameters of the clover fit are poorly determined, we do not consider them any further.

If, instead, we fit the data keeping points at $\beta \geq 6.0$, then

$$\begin{aligned} m_s(M_\phi) &= 105(21) \text{ MeV}[1 + 1.4(1.0) \text{ GeV } a] && \chi^2/dof = 0.3 && \text{Wilson} \\ m_s(M_\phi) &= 104(5) \text{ MeV}[1 - (0.74(14) \text{ GeV } a)^2] && \chi^2/dof = 1.8 && \text{Staggered} . \end{aligned} \quad (17)$$

For our best estimate of $m_s(M_\phi)$ in the quenched theory we average the Wilson and staggered values given in Eqs. 16 and 17

$$m_s(\overline{MS}, \mu = 2 \text{ GeV}, M_\phi) = 100(21) \text{ MeV} \quad \text{(quenched)}. \quad (18)$$

where we quote the largest of the extrapolation errors.

The $n_f = 2$ data for $m_s(M_\phi)$ are shown in Fig. 7. In light of the discussion presented in Section 5 and 8 we only consider data with $\beta \geq 5.5$. Furthermore, the spread between the values of m_s obtained by different collaborations at a given β are large, so we do not extrapolate assuming the expected $O(a)$ corrections. Instead we simply take the average in both cases. This gives $m_s = 76(10)$ MeV for the Wilson formulation and $m_s = 59(6)$ MeV for the staggered. For our final estimate in the $a = 0$ limit, we take the average of these two values,

$$m_s(\overline{MS}, \mu = 2 \text{ GeV}, M_\phi) = 68(12) \text{ MeV} \quad (n_f = 2), \quad (19)$$

where the spread in the data is taken to be representative of the uncertainty in the extrapolation to the continuum limit.

The estimates for m_s found using M_{K^*} match with $m_s(M_\phi)$ as exemplified in Fig. 6. To summarize, we find that the quenched estimate of m_s depends on the hadronic state (M_K versus M_ϕ or M_{K^*}) used to extract it. While the first estimate is constrained by the lowest order chiral perturbation theory, the second is an independent estimate. Thus, for our final estimates we take

$$m_s(\overline{MS}, \mu = 2 \text{ GeV}, M_\phi) = 100 \pm 21 \pm 10 \text{ MeV} \quad (\text{quenched}), \quad (20)$$

$$m_s(\overline{MS}, \mu = 2 \text{ GeV}, M_\phi) = 68 \pm 12 \pm 7 \text{ MeV} \quad (n_f = 2). \quad (21)$$

where the second error is the 10% uncertainty in setting the lattice scale as discussed in Section 8. Using these, one can again make a linear extrapolation in n_f to get $m_s \sim 55$ MeV for the three flavor theory. However, we feel that it is important to stress that the unquenched simulations are still in very early stages with respect to both statistical and systematic errors. Thus, unquenched estimates should be considered preliminary.

To summarize, the data show two consistent patterns. First, for a given value of a the $n_f = 2$ results are smaller than those in the quenched approximation. Second, the ratio $\overline{m}/m_s(M_\phi)$ is in good agreement with the predictions of chiral perturbation theory for both the $n_f = 0$ and 2 estimates. Quantitatively, our estimates are low and will be refined as data at more values of β , possibly with $n_f = 2 - 4$ to bracket the physical case of $n_f = 3$, become available.

7 STUDY OF THE CLOVER IMPROVEMENT

At $\beta = 6.0$ there now exist data at a number of values of the clover coefficient as listed in Table 6. This allows us to study the effect of improvement on quark masses as a function of c_{SW} in the range 0–3.0. Note that the value predicted by the Alpha Collaboration for $O(a)$ non-perturbative improvement is 1.769 [11]. The data, presented in Table 7, are plotted in Fig. 8 along with the Wilson and staggered fits reproduced from Fig. 1, and the staggered points at $\beta = 6.0$. Qualitatively, increasing the clover coefficient increases a and decreases \overline{m} . In particular, the scale at $c_{SW} = 1.769$ matches that from the staggered data. However, the value of \overline{m} is significantly ($\sim 50\%$) different. For a complete $O(a)$ improvement with clover actions, the lattice quark mass needs an $O(ma)$ correction, *i.e.* $m_q^{improved} = m_q(1 + b_m m_q a)$ where $b_m = -0.5$ at tree level [11]. This is, however, a few percent effect only for the parameter values we have analyzed. The other two possible explanations are the failure of perturbation theory used to determine Z_m , and possibly large $O(a^2)$ effects. More work, like determining Z_m non-perturbatively, is required to quantify these effects.

Table 6: Lattice parameters of the runs at $\beta = 6.0$ for different values of the clover coefficient in the Sheikholeslami-Wohlert action.

Label	Ref.	c_{SW}	Lattice size	# of Conf.	Quark masses used in the fits	Scale $1/a$ (GeV)	$\alpha_{\overline{MS}}(q^*)$ ($1/a$)	$\alpha_{\overline{MS}}(q^*)$ (2 GeV)
W8	[22]	0	$32^3 \times 64$	170	0.155, 0.1558, 0.1563	2.338(43)	0.192	0.205
C1	[27]	1.0	$18^3 \times 64$	200	0.1425, 0.1432, 0.1440	1.867(81)	0.192	0.187
C5	[41]	1.4785	$32^3 \times 64$	100	0.13808, 0.13851, 0.13878	2.028(96)	0.192	0.193
C6	[42]	1.769	$24^3 \times 64$	100	0.1342, 0.1346, 0.1348	1.762(78)	0.192	0.184
C7	[42]	1.92	$16^3 \times 32$	100	0.1290, 0.1300, 0.1310, 0.1320	1.734(26)	0.192	0.182
C8	[42]	2.25	$16^3 \times 32$	100	0.1260, 0.1265, 0.1270, 0.1277	1.695(42)	0.192	0.181
C9	[42]	3.0	$16^3 \times 32$	100	0.1160, 0.1165, 0.1170, 0.1173	1.594(48)	0.192	0.177

Table 7: The results for the quenched simulations using the Sheikholeslami-Wohlert action as listed in Table 6. The notation is the same as in Table 4.

Label	κ_c	B_π	A_ρ	B_ρ	\overline{m}		$m_s(M_\phi)$	
					$\overline{m}a \times 10^5$	\overline{m}	$m_s a \times 10^3$	m_s
W8	0.157143(03)	1.993(26)	-6.663(521)	2.196(162)	172(06)	5.20(11)	50(05)	152(11)
C1	0.145483(03)	2.674(29)	-6.265(1006)	1.942(288)	201(18)	5.33(24)	71(13)	188(27)
C5	0.139285(01)	2.837(50)	-9.913(2491)	2.866(689)	161(15)	4.89(24)	45(12)	136(32)
C6	0.135222(05)	3.268(126)	-7.318(2973)	2.096(799)	185(17)	4.87(27)	70(29)	183(68)
C7	0.133062(05)	3.483(20)	-8.914(243)	2.489(63)	179(05)	4.67(07)	60(02)	156(4)
C8	0.128536(07)	3.640(50)	-9.934(673)	2.669(170)	179(09)	4.64(12)	57(05)	147(9)
C9	0.118151(104)	3.906(195)	-13.101(714)	3.209(166)	189(10)	4.67(19)	51(04)	125(6)

8 ANALYSIS OF SYSTEMATIC ERRORS

We have checked the validity of our analysis ignoring correlations between data by comparing results presented here against those obtained from a detailed error analysis using the quenched Wilson data obtained on $170\ 32^3 \times 64$ lattices at $\beta = 6.0$ [22]. For example, in Ref. [22], we quote $m_s(M_\phi) = 154(8)\ MeV$, whereas the current analysis gives $152(11)$, the number plotted in Fig. 5. A similar agreement is seen if we compare our estimates with the results of the original analysis by collaborations whose data we have used as discussed in Section 9. Thus, we believe that the analysis presented here gives central values in the individual points reliable to within a few percent, and the estimate of statistical errors to within a factor of two.

There is accumulating evidence in high statistics data that fits linear in the quark mass, Eq. 11, are not sufficient, *i.e.* chiral logs and terms of higher order in m need to be included [9, 40, 43]. (Chiral perturbation theory for pseudoscalar mesons does not indicate any large non-linearities as the change in m_s/\overline{m} and m_u/m_d between the lowest and next order analyses is insignificant [4].) In a state-of-the-art quenched calculation presented in Ref. [22], we found that including higher order terms in the fits for pseudoscalar and vector mesons changes the estimates of quark masses by less than a few percent. In the present study we have not carried out this detailed analysis because in most of the data the quality of statistical precision and the number of values of light quark masses simulated are insufficient to uncover these effects. The deviations from linearity are found to be smaller for pseudoscalar mesons, which is another reason why we used them to fix \overline{m} , and vector mesons to fix m_s . In short, even though present lattice data does not rule out the possibility of large systematic errors due to the neglected higher order terms, there is no clear indication that this is the case. This issue can be addressed only when the range of quark masses used in the fits is increased.

For Wilson and clover type of fermions, the errors in the calculation of κ_c and the κ corresponding to light quarks is highly correlated. As a result the estimate of errors in $1/2\kappa - 1/2\kappa_c$ is much smaller, and we find that the low statistics points give estimates that are consistent with the high statistics large lattice data. Thus we believe that the estimate, in the $a = 0$ limit, will not change significantly on improving just the statistical quality of the current data. What is more important is to increase the range of quark masses in the chiral fits and to verify whether the lowest order correction formulae used in the extrapolation to $a = 0$ are sufficient. We have partially addressed the second issue by comparing the continuum limit of data from different lattice actions. We plan to test these issues in the future as data at smaller m_q and a become available.

The clover action with $c_{SW} = 1.0$ has discretization errors starting at $O(\alpha_s a)$ and it is not known whether $O(\alpha_s a)$ or $O(a^2)$ errors dominate for $\beta \geq 6.0$. Nevertheless, one would have expected the corrections to be smaller than those for Wilson fermions. However, the current data show a near agreement between Wilson and clover data. With data at just three values of coupling it is hard to determine what form to use to extrapolate the clover action data to the continuum limit. The most we can say is that using a linear extrapolation, a theoretically allowed form, gives results consistent with the rest of our analysis.

The lattice scale a : The value of the lattice scale a enters into the calculation in two ways. It is used to convert the dimensionless lattice quantity ma into physical units. A much weaker dependence arises when matching the lattice and continuum theories. This is because one specifies the renormalization point μ , at which the lattice and continuum theories are matched, in terms of $1/a$. Present lattice data show a considerable spread in the determination of a depending on the physical quantity used. This variation is due to a combination of discretization and quenching errors. For example, with our high statistics quenched Wilson data [22], we have calculated the lattice

scale fixing M_ρ , f_π , and M_N to their physical values. The results are $1/a(M_\rho) = 2.330(41)$ GeV, $1/a(f_\pi) = 2.265(57)$ GeV, and $1/a(M_N) = 2.062(56)$ GeV [22]. Also, the fluctuations between the determination of scale at a given β by the different groups (see Tables 2, 3, 6) are of the same magnitude. Thus, using M_ρ to set the scale could lead to an additional 10% uncertainty in our estimates of quark masses, which we quote as a separate error in our final estimates.

The $n_f = 2$ Wilson data: We show the data for $\beta \geq 5.3$ obtained on $16^3 \times 32$ lattices in Fig. 9. We highlight the highest statistics points by the symbol octagon. The striking feature of this data is the surprisingly low value $\overline{m} \approx 1.1$ MeV at $\beta = 5.3$. Coincidentally, the SCRI collaboration has reported an anomalous behavior in the calculation of the non-perturbative β -function at $\beta = 5.3$ [36]. The important question is whether this is an anomalous measurement or is indicative of a serious problem. If this feature is borne out by future calculations, then one possible interpretation is that the lattice theory has a phase transition close to $\beta = 5.3$, similar to that seen in the fundamental-adjoint coupling plane of the pure gauge model. Such singular points are lattice artifacts, and to avoid their influence in the extrapolation to $a = 0$ one has to consider data at weaker coupling or improve the action to stay away from such singularities. In the former case one would need to consider data at couplings weaker than $\beta = 5.3$. Motivated by the need to minimize contamination from such effects, we have chosen to use data at $\beta \geq 5.5$ only.

The above scenario would also explain why the Wilson data for $\beta \leq 5.5$ ($a > 0.42$ GeV $^{-1}$) appear to lie marginally below the staggered data, in contrast to the quenched estimates. Furthermore, one might worry about the presence of such artifacts at even weaker coupling. In the long run such a possibility is addressed by our strategy of demanding agreement, in the $a = 0$ limit, of results obtained using different lattice discretizations of the Dirac action since the presence and influence of such artifacts depend on the lattice action.

9 COMPARISON WITH PREVIOUS ESTIMATES

The ROME/APE collaboration quotes the value $m_s(M_K) = 128(18)$ MeV [12] from their quenched simulations. Their estimate is based on an analysis of data obtained using both the Wilson and the clover actions at $\beta = 6.0$ and 6.2 , but does not include a linear extrapolation to $a = 0$. Their number is consistent with the result $128(4)$ MeV reported by us in Ref. [22]. However, our present analysis of the global data show the presence of large $O(a)$ corrections for the Wilson theory. Including this correction results in a much lower number, $m_s(M_K) = 88(10)$ MeV, after extrapolation to $a = 0$ as shown in Fig. 4.

The APE collaboration has recently updated their estimates using data with Wilson and Clover actions at $\beta = 6.0, 6.2, 6.4$ [27]. These data are included in our analysis and we agree with the raw numbers. However, they quote the value $m_s(\overline{MS}, 2 \text{ GeV}, M_K) = 122(20)$ MeV, based on taking an average of the data rather than doing an extrapolation in a . Since they only analyze their own data, they are not able to make a case for linear extrapolation as advocated by us.

Gough *et al.* [44] have also presented results for both the Wilson and clover actions for $\beta = 5.7, 5.9, 6.1$. Even though their values for $\overline{m}(\overline{MS}, 2 \text{ GeV})$ at a given β are systematically lower than what we find due to the differences between the two analyses in determining a , their estimates of the continuum values are consistent with the results presented here.

The analysis by Lee of the $n_f = 2$ staggered data generated by the Columbia collaboration at $\beta = 5.7$ yielded $\overline{m} = 2.7$ MeV [45]. This is consistent with $2.62(9)$, the result of our analysis of their data, and with the value, $2.95(14)$ MeV, we get for the data by Fukugita *et al.* [38] at the same coupling.

To conclude, the values of quark masses that we have extracted at a given lattice scale are consistent with previous analysis. Both the central value and the error estimates based on our simple analysis are consistent with the previous analysis once the differences in the regularization schemes are taken into account. The main new feature of our analysis is to show that the data roughly follow the expected $O(a)$ corrections for quenched Wilson and clover fermions and $O(a^2)$ for staggered. We also show that including these corrections give results that are consistent between the various discretization schemes.

10 IMPACT ON ϵ'/ϵ

The Standard Model (SM) prediction of ϵ'/ϵ can be written as [46]

$$\epsilon'/\epsilon = A \left\{ c_0 + [c_6 B_6^{1/2} + c_8 B_8^{3/2}] M_r \right\}, \quad (22)$$

where $M_r = (158 \text{ MeV}/(m_s + m_d))^2$ and all quantities are to be evaluated at the scale $m_c = 1.3 \text{ GeV}$. This form highlights the dependence on the light quark masses and the B parameters. For central values of the SM parameters quoted by Buras *et al.* [46], we estimate $A = 1.29 \times 10^{-4}$, $c_0 = -1.4$, $c_6 = 7.9$, $c_8 = -4.0$. Thus, to a good approximation $\epsilon'/\epsilon \propto M_r$; and increases as $B_8^{3/2}$ decreases. Conventional analysis, with $m_s + m_d = 158 \text{ MeV}$ and $B_6^{1/2} = B_8^{3/2} = 1$, gives $\epsilon'/\epsilon \approx 3.2 \times 10^{-4}$. On the other hand taking $m_s + m_d \approx 85 \text{ MeV}$, our $n_f = 2$ estimates scaled to m_c , and $B_8^{3/2} = 0.8$ [20] gives $\epsilon'/\epsilon \approx 19 \times 10^{-4}$. This estimate lies in between the Fermilab E731 $(7.4(5.9) \times 10^{-4})$ [47] and CERN NA31 $(23(7) \times 10^{-4})$ [48] measurements. Since the new generation of experiments will reduce the uncertainty to 1×10^{-4} , tests of the enhanced value are imminent.

11 Continuum limit of the Quark Condensate

The observation that the present lattice data for pseudoscalar mesons is well described by $M_\pi^2 = B_\pi m_q$ allows us to calculate the chiral condensate using the Gell-Mann-Oakes-Renner relation [2, 49]

$$\langle \bar{\psi}\psi \rangle^{\text{GMOR}} = \lim_{m_q \rightarrow 0} -\frac{f_\pi^2 M_\pi^2}{4m_q}. \quad (23)$$

Since $m_q \langle \bar{\psi}\psi \rangle$ is renormalization group invariant, we analyze the slope of M_π^2 versus the renormalized mass at a fixed scale, *i.e.* $m_q(\overline{MS}, 2 \text{ GeV})$, for the data sets described in Tables 2 and 3. The slope, after extrapolation to $a = 0$, directly give an estimate of $4\langle \bar{\psi}\psi \rangle/f_\pi^2$ in \overline{MS} scheme at $\mu = 2 \text{ GeV}$. Our results for the quenched and dynamical configurations are displayed in Figs. 10 and 11 respectively. The fits, assuming a linear behavior in a for Wilson and clover and a^2 for staggered fermion formulations, to the quenched data with $\beta \geq 6.0$ give

$$\frac{-4\langle \bar{\psi}\psi \rangle}{f_\pi^2} = 5.41(12) \text{ GeV}[1 - 0.72(7) \text{ GeV } a] \quad \chi^2/dof = 2.6 \text{ (Wilson } n_f = 0) \quad (24)$$

$$\frac{-4\langle \bar{\psi}\psi \rangle}{f_\pi^2} = 5.64(15) \text{ GeV}[1 - 0.73(6) \text{ GeV } a] \quad \chi^2/dof = 12.1 \text{ (clover } n_f = 0) \quad (25)$$

$$\frac{-4\langle \bar{\psi}\psi \rangle}{f_\pi^2} = 6.13(3) \text{ GeV}[1 - (0.46(2) \text{ GeV } a)^2] \quad \chi^2/dof = 19.5 \text{ (staggered } n_f = 0) \quad (26)$$

The fits for clover and staggered data do not work. In particular, the staggered data show a break at $\beta \approx 6.0$. At weaker coupling the data lie in the band 5.9(2) showing no clear a dependence. Taking this to be the best estimate for staggered fermions, we find that the three values are in rough agreement. Thus, for our final value we take the mean of these, *i.e.* $4\langle\bar{\psi}\psi\rangle/f_\pi^2 = 5.7(4)$ GeV, where the error covers the spread. Using the experimental value of $f_\pi = 131\text{MeV}$, we then obtain

$$\langle\bar{\psi}\psi\rangle = -0.024 \pm 0.002 \pm 0.002 \text{ GeV}^3 \quad (27)$$

$$m_s\langle\bar{\psi}\psi\rangle = -0.0023 \pm 0.0006 \pm 0.0004 \text{ GeV}^4 \quad (28)$$

as our estimate for the quenched theory. The second error arises from the 10% scale uncertainty discussed in section 8.

The behavior of the dynamical data is again not clear. Therefore, we take the average 7.3(1.0) of the values at the weakest coupling as our best estimate. This gives

$$\langle\bar{\psi}\psi\rangle = -0.031 \pm 0.004 \text{ GeV}^3 \quad (29)$$

$$m_s\langle\bar{\psi}\psi\rangle = -0.0021 \pm 0.0006 \text{ GeV}^4. \quad (30)$$

The corresponding phenomenological estimates are [2]

$$\langle\bar{\psi}\psi\rangle = -0.0114 \text{ GeV}^3 \quad (31)$$

$$m_s\langle\bar{\psi}\psi\rangle = -0.0017 \text{ GeV}^4. \quad (32)$$

Thus, lattice estimates give low values for the quark masses and correspondingly high values for the condensate, while roughly preserving $m\langle\bar{\psi}\psi\rangle$.

12 CONCLUSIONS:

We have presented an analysis of \bar{m} and m_s using data generated by us over the years and also by other collaborations. The values of quark masses we have extracted for a given set of lattice parameters are consistent with previous analyses. Both the central value and the error estimates we get by reanalyzing the data are consistent with the previous reported results once the differences in the regularization schemes are taken into account. The main new feature of our work, based on the global analysis, is to show that the data roughly follow the expected $O(a)$ corrections for Wilson fermions and $O(a^2)$ for staggered. The errors in the clover action are expected to be $O(a/\log(a))$, however over the limited range of a it is not surprising that the present data is consistent with a linear fit. What is surprising is that the $O(a)$ corrections are still as large as for Wilson fermions. The bottom line is that including these corrections give results that are consistent between the three discretization schemes after extrapolation to the continuum limit.

We quote our final results in the \overline{MS} scheme evaluated at $\mu = 2$ GeV. The lattice perturbation theory is reorganized using the Lepage-Mackenzie scheme. Our best estimate of the isospin symmetric mass \bar{m} is $3.4 \pm 0.4 \pm 0.3$ MeV for the quenched theory. For the $n_f = 2$ flavors there does not exist enough data to extrapolate to the continuum limit. The mean of the data at weakest couplings gives $\bar{m}(\overline{MS}, 2 \text{ GeV}) = 2.7 \pm 0.3 \pm 0.3$ MeV. Using a linear extrapolation in n_f would give $\bar{m} \sim 2.4$ MeV for the physical case.

To extract the value of m_s we use the physical value of M_ϕ (or equivalently M_{K^*}). Using M_K instead constrains $m_s(M_K) = 25.9\bar{m}$ since we use a linear fit to the pseudoscalar mass data. Our best estimate for the quenched theory is $m_s(\overline{MS}, \mu = 2 \text{ GeV}, M_\phi) = 100 \pm 21 \pm 10$ MeV, and

$68 \pm 12 \pm 7$ MeV for the two flavor case. The variation with n_f would again suggest an even smaller value for the physical $n_f = 3$ theory, however, we caution the reader that the unquenched simulations are still in infancy.

In short, taking into account the various systematic errors, like allowing for a 10% uncertainty in the estimates due to the uncertainty in setting the lattice scale a , the present lattice results for both \overline{m} and m_s are surprisingly low compared to the numbers used in phenomenology, *i.e.* $\overline{m} = 6-7$ MeV and $m_s = 150 - 175$ MeV. The main uncertainty in the lattice results arises due to lack of control over the extrapolation of the two flavor data to the continuum limit, and consequently the final extrapolation to $n_f = 3$. To address these issues requires unquenched data at more values of β . The data suggest that, with respect to statistical and discretization errors, the better approach is to use staggered fermions, however one has to confront the issue of a large Z_m . On the other hand one needs to understand why the non-perturbatively improved Sheikholeslami-Wohlert action has large discretization errors. Clearly, the reliability of these estimates will be improved in the next few years as more data become available.

From a study of the variation of the pseudoscalar data as a function of the quark mass we also extract the quantity $\langle \overline{\psi}\psi \rangle / f_\pi^2$ using the Gell-Mann-Oakes-Renner relation. After taking the continuum limit we find that the chiral condensate is roughly a factor of two larger than phenomenological estimates. Consequently, the estimate of the renormalization group invariant quantity $m\langle \overline{\psi}\psi \rangle$ is preserved.

13 Acknowledgements

The simulations carried out by our collaboration have been done on the Crays at NERSC, and on the CM2 and CM5 at LANL as part of the DOE HPCC Grand Challenge program, and at NCSA under a Metacenter allocation. We thank Jeff Mandula, Larry Smarr, Andy White and the entire staff at the various centers for their tremendous support throughout this project. We also thank Chris Allton, Shoji Hashimoto, Urs Heller, Thomas Lippert, Don Sinclair, and Akira Ukawa for communicating some of their unpublished data to us. We are grateful to Eduardo de Rafael for discussions on the sum-rule analysis, and to Steve Sharpe for his comments.

References

- [1] Review of Particle Properties, Phys. Rev. **D50** (1994) 1173.
- [2] J. Gasser and H. Leutwyler, Phys. Rep. **C87** (1982) 77.
- [3] H. Leutwyler, Nucl. Phys. **B337** (1990) 108.
- [4] H. Leutwyler, hep-ph/9609467.
- [5] J. Bijnens, J. Prades, and E. de Rafael, Phys. Lett. **348B** (1995) 226.
- [6] M. Jamin and M. Münz, Z. Phys. **C66** (1995) 633.
- [7] T. Bhattacharya, R. Gupta, and K. Maltman, hep-ph/9703455.
- [8] A. Ukawa, LATTICE92, Nucl. Phys. (Proc. Suppl.) **B30** (1992) 3.
- [9] R. Gupta, Nucl. Phys. (Proc. Suppl.) **B42** (1995) 85.
- [10] B. Sheikholeslami and R. Wohlert, Nucl. Phys. **B259** (1985) 572.
- [11] M. Lüscher, S. Sint, R. Sommer, and P. Weisz, hep-lat/9605038
- [12] C. R. Allton, *et al.*, APE collaboration, Nucl. Phys. **B431** (1994) 667.
- [13] T. Bhattacharya and R. Gupta, in preparation.
- [14] G. Martinelli and Z. Yi-Cheng, Phys. Lett. **123B** (1983) 433.
- [15] M. Golterman and J. Smit, Phys. Lett. **140B** (1984) 392.
- [16] M. Göckeler, *et al.*, Nucl. Phys. (Proc. Suppl.) **B53** (1997) 896; hep-lat/9608033.
- [17] P. Lepage and P. Mackenzie, Phys. Rev. **D48** (1993) 2250.
- [18] K. Bitar, *et al.*, HEMCGC collaboration, Phys. Rev. **D46** (1992) 2169.
- [19] K. Bitar, *et al.*, HEMCGC collaboration, Phys. Rev. **D49** (1994) 6026.
- [20] R. Gupta, T. Bhattacharya, and S. Sharpe, Phys. Rev. **D55** (1997) 4036; LAUR-96-1829, hep-lat/9611023
- [21] T. Bhattacharya, D. Daniel, and R. Gupta, LAUR-93-3580, hep-lat/9310007
- [22] T. Bhattacharya, R. Gupta, G. Kilcup, and S. Sharpe, Phys. Rev. **D53** (1996) 6486.
- [23] S. Cabasino, *et al.*, APE collaboration, Phys. Lett. **258B** (1991) 195; A. Abada, *et al.*, ELC collaboration, Nucl. Phys. **B376** (1992) 172; M. Guagnelli, *et al.*, APE collaboration, Nucl. Phys. **B378** (1992) 616.
- [24] A. Aoki, *et al.*, JLQCD Collaboration, Nucl. Phys. (Proc. Suppl.) **B53** (1997) 209; hep-lat/9608144.
- [25] F. Butler, *et al.*, GF11 Collaboration, Nucl. Phys. **B430** (1994) 179.
- [26] Y. Iwasaki, *et al.*, QCDPAX collaboration, Phys. Lett. **216B** (1989) 387, Phys. Rev. **D53** (1996) 6443.
- [27] C.R.Allton, V.Giménez, L.Giusti and F.Rapuano, Nucl. Phys. **B489** (1997) 427, hep-lat/9611021.
- [28] C. Allton, *et al.*, UKQCD collaboration, Nucl. Phys. **B407** (1993) 331.
- [29] P. Bacilieri, *et al.*, APE collaboration, Nucl. Phys. **B343** (1990) 228; S. Cabasino, *et al.*, APE collaboration, Phys. Lett. **258B** (1991) 202.

- [30] A. Aoki, *et al.*, JLQCD Collaboration, private communications.
- [31] R. Gupta, G. Guralnik, G. Kilcup, and S. Sharpe, Phys. Rev. **D43** (1991) 2003. G. Kilcup, Nucl. Phys. (Proc. Suppl.) **B34** (1994) 350.
- [32] S. Kim and D. Sinclair, Phys. Rev. **D48** (1993) 4408, and private communications.
- [33] S. Kim and S. Ohta, Nucl. Phys. (Proc. Suppl.) **B53** (1997) 199; hep-lat/9609023.
- [34] R. Gupta, C. Baillie, R. Brickner, G. Kilcup, A. Patel, and S. Sharpe, Phys. Rev. **D44** (1991) 3272.
- [35] K. Bitar, *et al.*, HEMCGC Collaboration, Phys. Rev. **D49** (1994) 3546.
- [36] K. M. Bitar, R. G. Edwards, U. M. Heller, and A. D. Kennedy, Phys. Rev. **D54** (1996) 3546, hep-lat/9607043, and private communications.
- [37] U. Glässner, SESAM Collaboration, Nucl. Phys. (Proc. Suppl.) **B53** (1997) 219; hep-lat/9608083.
- [38] M. Fukugita *et al.*, Tsukuba Collaboration, Phys. Rev. **D47** (1993) 4739, and S. Aoki, *et al.*, Phys. Rev. **D50** (1994) 486.
- [39] F. Brown, *et al.*, Columbia Collaboration, Phys. Rev. Lett. **67** (1991) 1062.
- [40] S. Sharpe, hep-lat/9609029.
- [41] T. Bhattacharya and R. Gupta, in preparation.
- [42] M. Göckeler, *et al.*, Phys. Lett. **391B** (1997) 388; hep-lat/9609008
- [43] For a recent review see S. Gottlieb, Nucl. Phys. (Proc. Suppl.) **B53** (1997) 155; hep-lat/9608107.
- [44] B. Gough, *et al.*, hep-ph/9610223.
- [45] W. Lee Nucl. Phys. (Proc. Suppl.) **B34** (1994) 396.
- [46] A. Buras, M. Jamin, and M. E. Lautenbacher, Phys. Lett. **389B** (1996) 749; hep-ph/9608365.
- [47] L. K. Gibbons, *et al.*, Phys. Rev. Lett. **70** (1993) 1203.
- [48] G. D. Barr, *et al.*, Phys. Lett. **317B** (1993) 233.
- [49] M. Gell-Mann, R.J. Oakes, and B. Renner, Phys. Rev. **175** (1968) 2195.

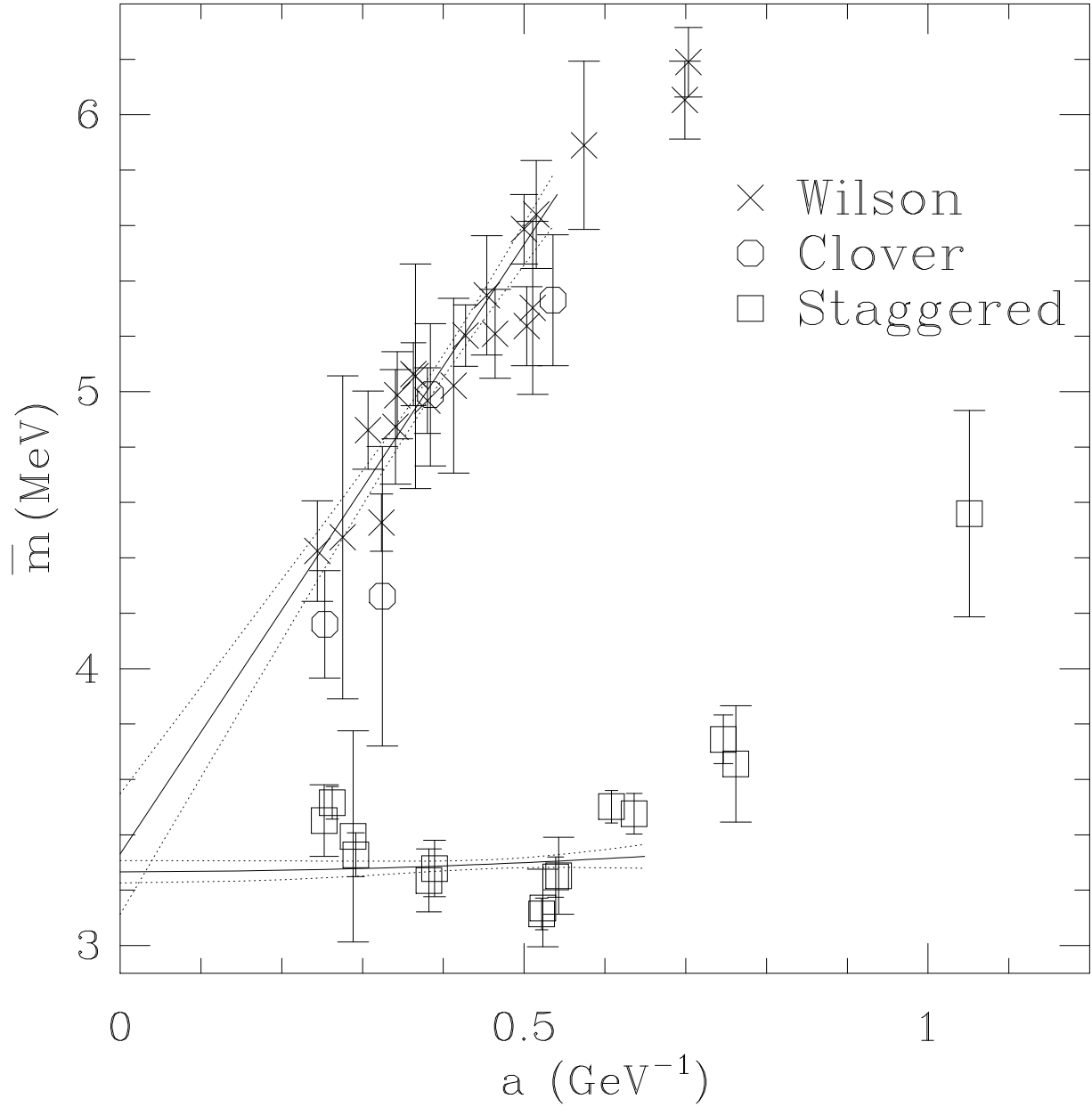


Figure 1: The behavior of $\bar{m}(\overline{MS}, 2 \text{ GeV})$ extracted using the quenched M_π data in the TAD1 lattice scheme defined in the text. The scale is set by M_ρ . We do not show the fit to the clover data for clarity.

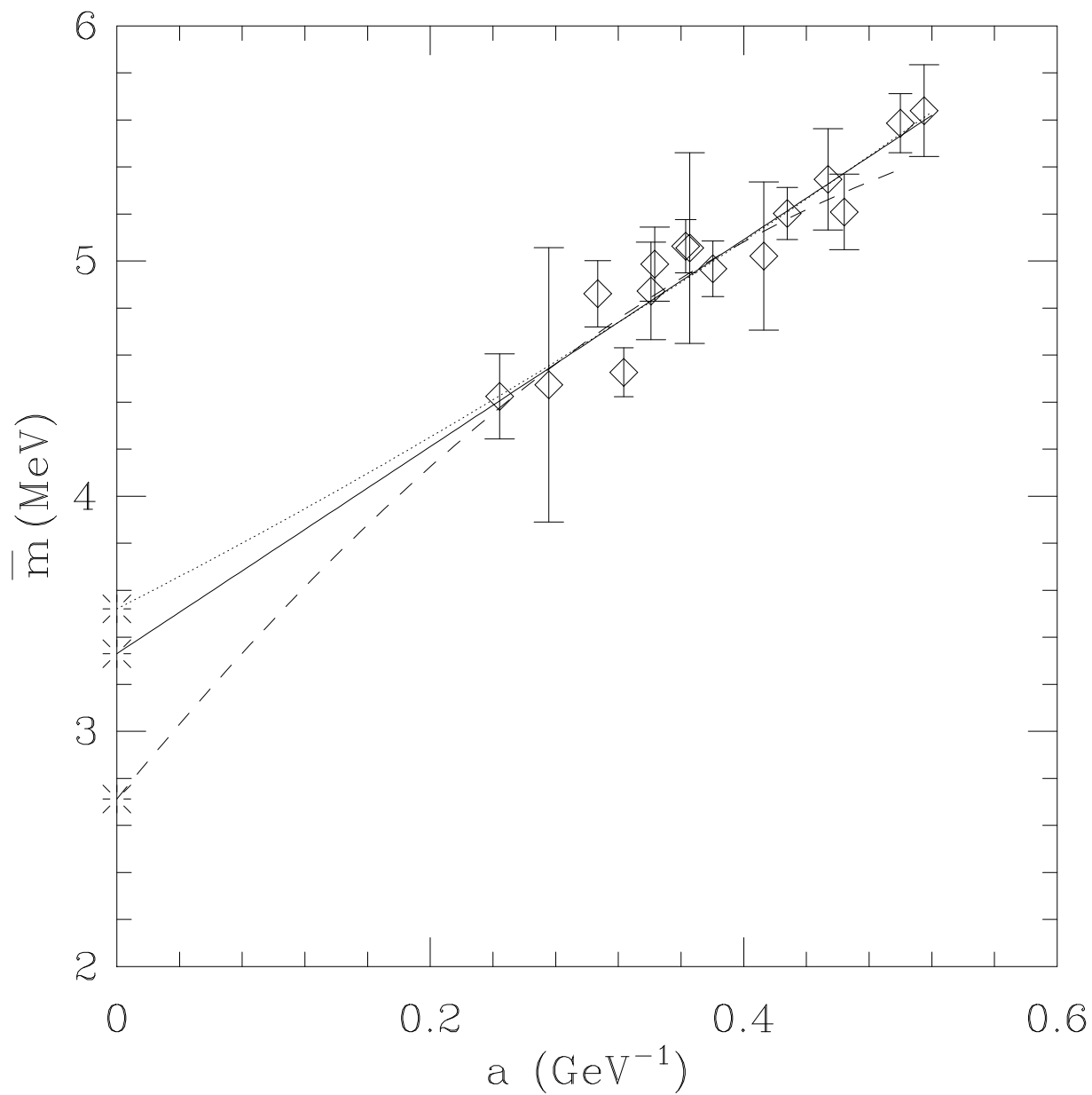


Figure 2: Three different fits to quenched Wilson data for $\overline{m}(\overline{MS}, 2 \text{ GeV})$. The solid line is a linear fit to points at $\beta \geq 5.93$, while the dotted line includes a quadratic correction. The dashed line is the quadratic fit to points at $\beta \geq 6.0$.

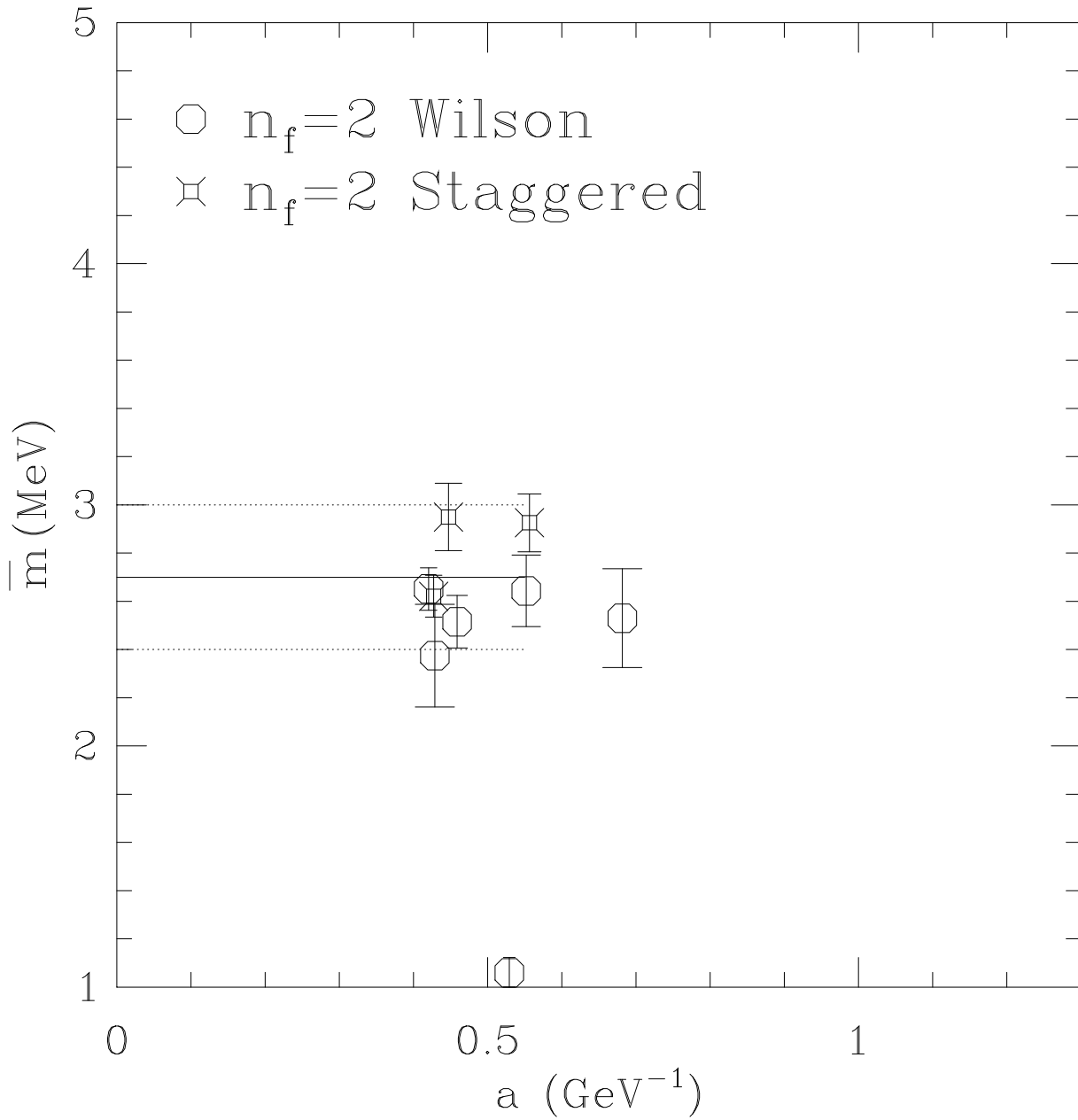


Figure 3: The behavior of $\bar{m}(\overline{MS}, 2 \text{ GeV})$, extracted using M_π data for $n_f = 2$ simulations. The scale is set by M_ρ , and the lattice scheme is TAD1.

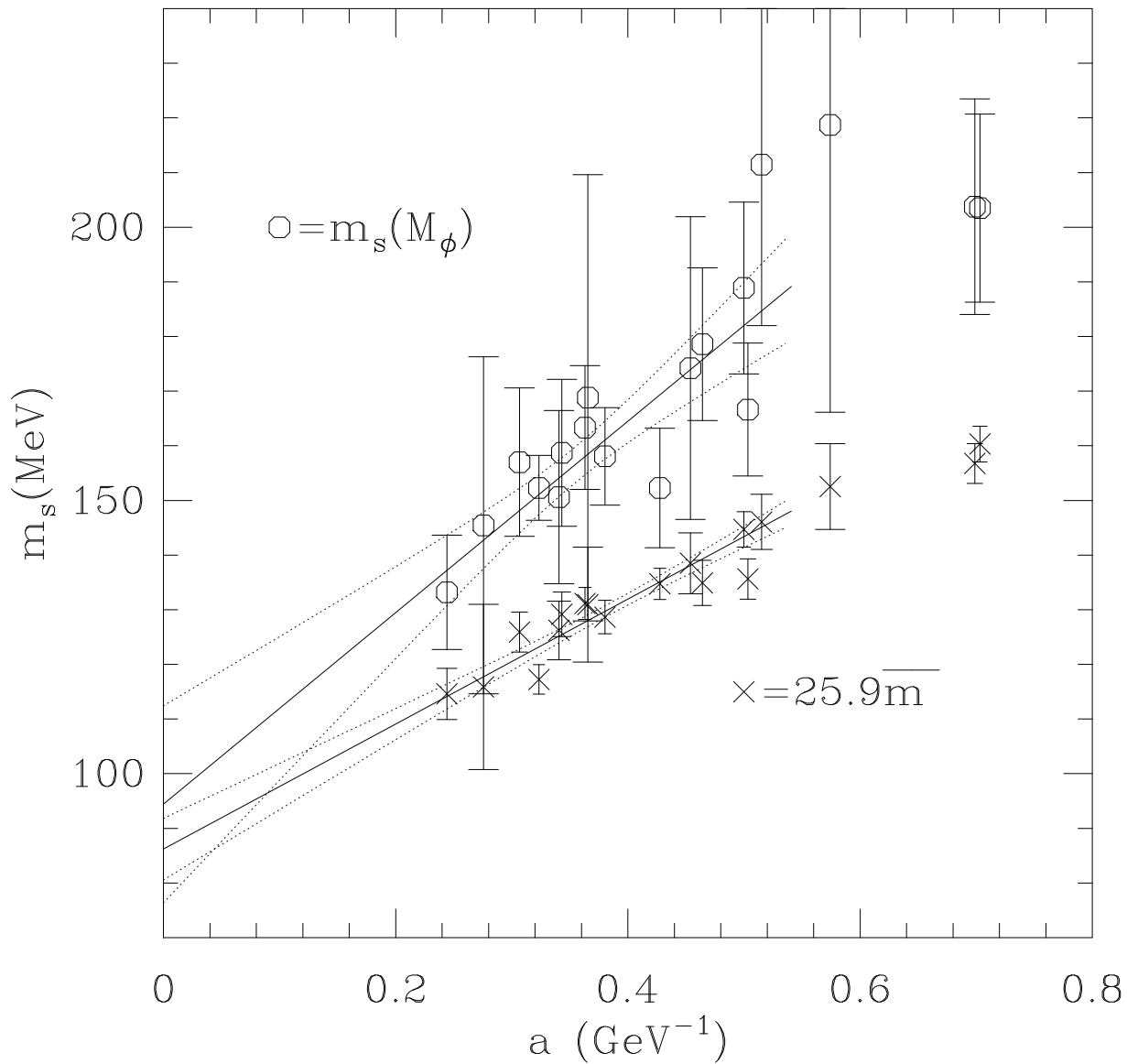


Figure 4: Comparison of $m_s(\overline{MS}, 2 \text{ GeV})$ extracted using M_ϕ against the lowest order chiral prediction $m_s = 25.9\overline{m}$. The data are for the quenched Wilson theory.

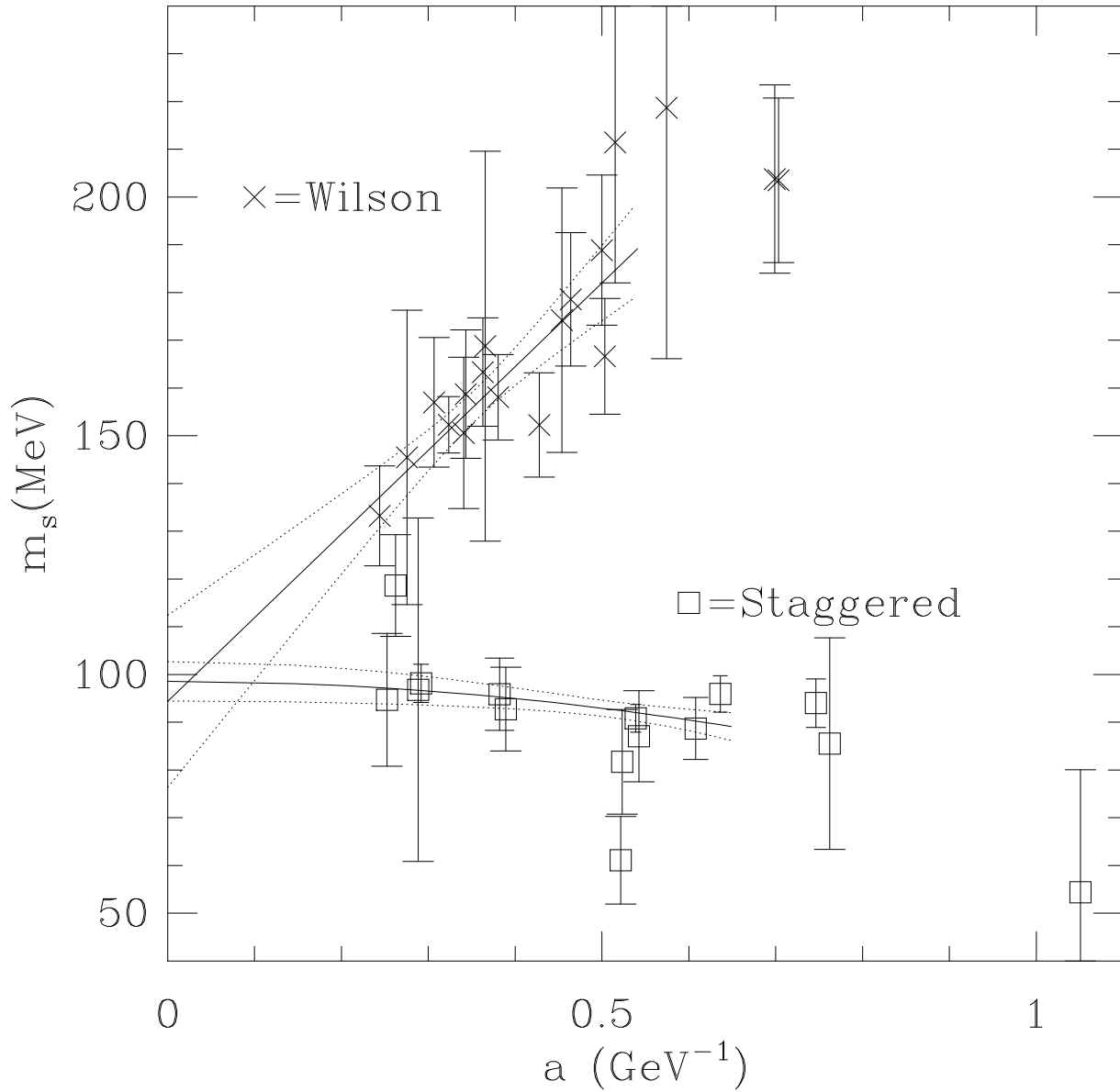
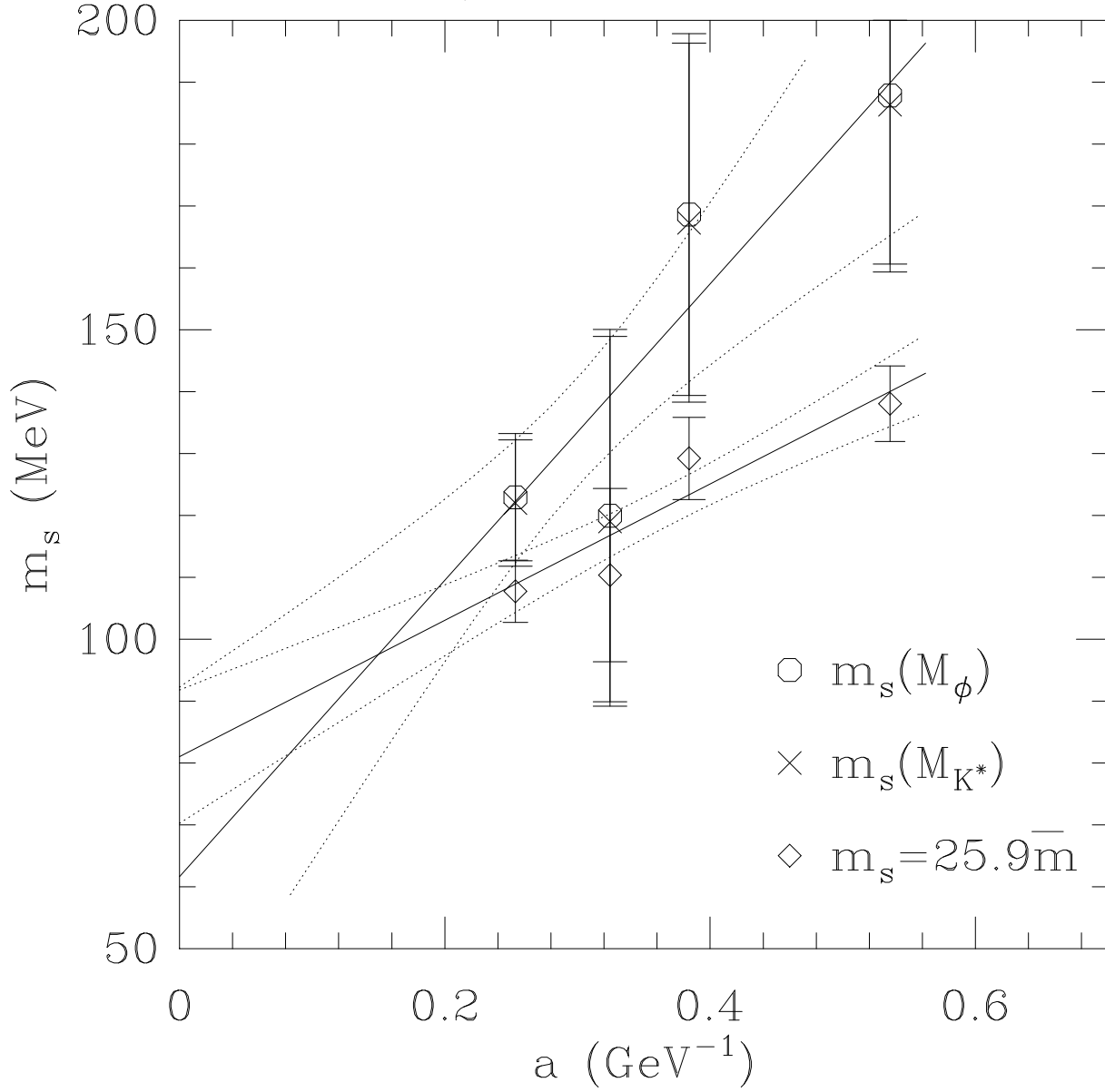


Figure 5: Comparison of $m_s(\overline{MS}, 2 \text{ GeV})$ extracted using M_ϕ for the quenched Wilson, and staggered theories.

Figure 6: Results for $m_s(\overline{MS}, 2 \text{ GeV})$ extracted using M_K , M_{K^*} , and M_ϕ for the quenched Clover action with tree-level value $c_{SW} = 1$ for the clover coefficient. The results for $m_s(M_\phi)$ and $m_s(M_{K^*})$ agree. We show linear fits to the $m_s(M_\phi)$ and $m_s(M_K)$ data.



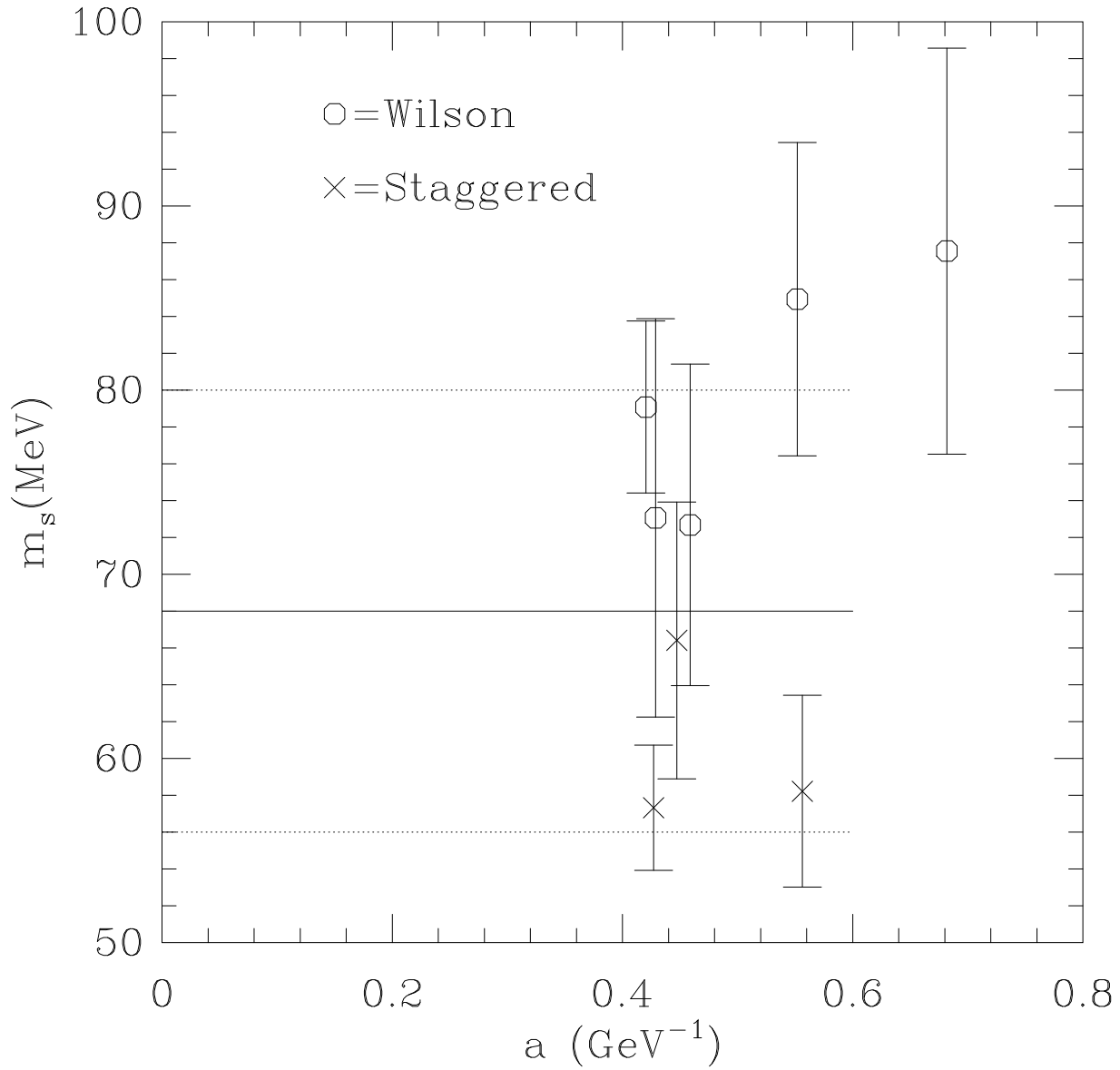


Figure 7: Comparison of $m_s(\overline{MS}, 2 \text{ GeV})$ extracted using M_ϕ for the $n_f = 2$ Wilson and staggered actions. The lines show the average value and the uncertainty in the estimate for the two formulations.

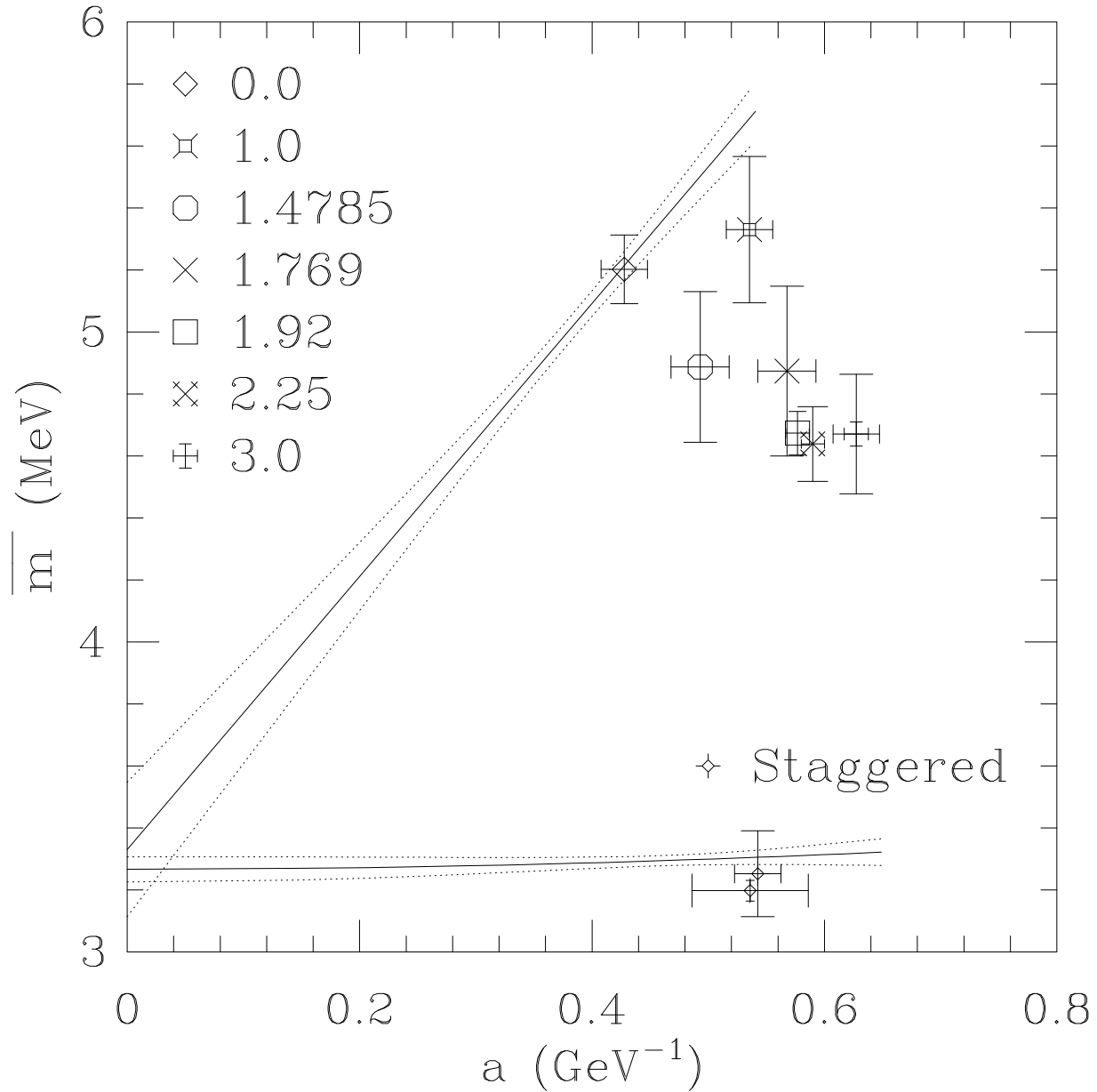


Figure 8: Behavior of $\bar{m}(\overline{MS}, 2 \text{ GeV})$ versus scale a as a function of the clover coefficient c_{SW} . We also reproduce the fits to the Wilson and staggered data, and the staggered result at $\beta = 6.0$ from Fig. 1 for comparison.

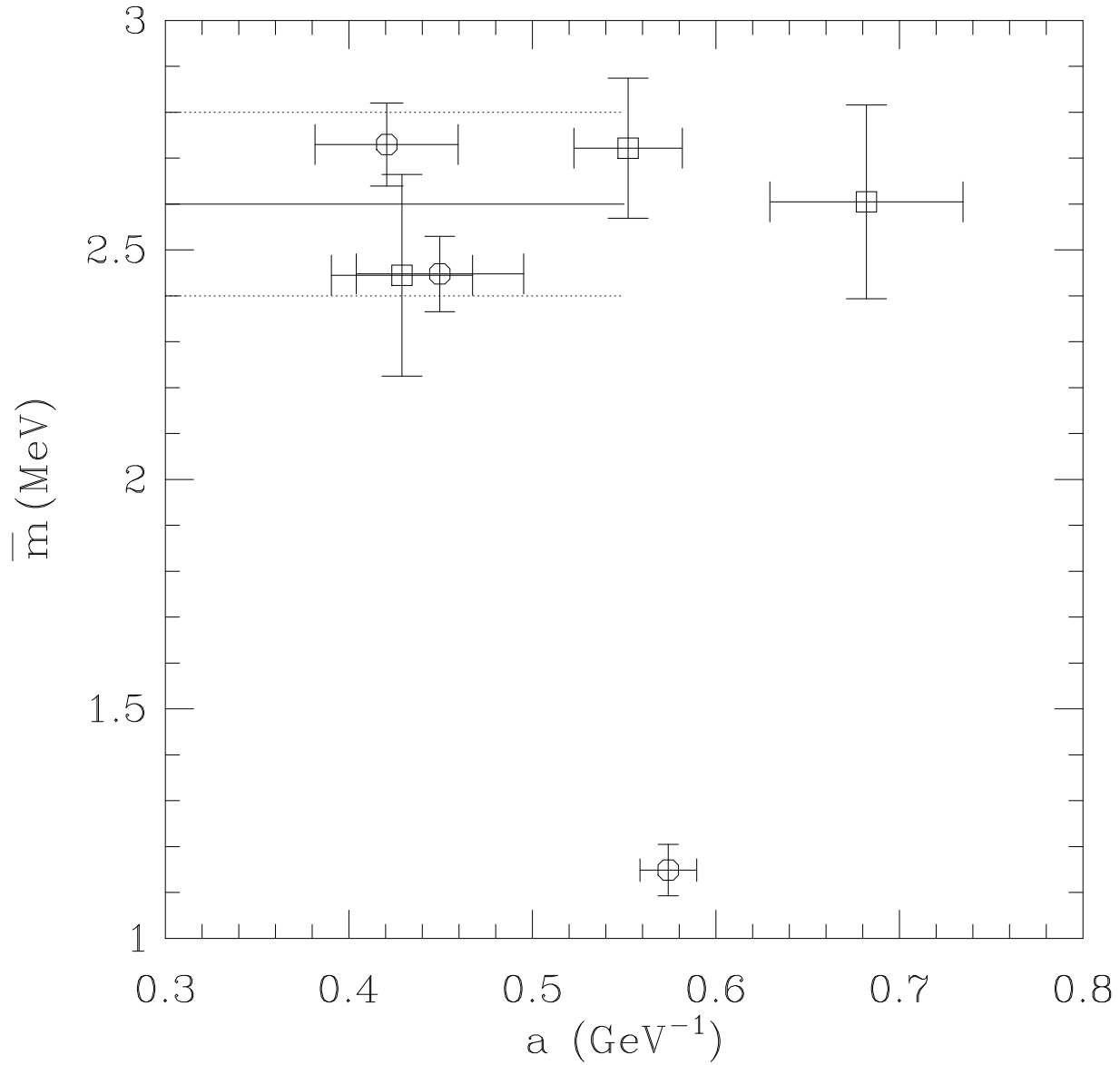


Figure 9: The $n_f = 2$ data for Wilson fermions. We show the highest statistics points at $\beta = 5.3, 5.5, 5.6$ with the symbol octagon. The remaining points are shown by the symbol square. We also plot our estimate, the average value for $\beta \geq 5.5$, and show the errors in a for each data point.

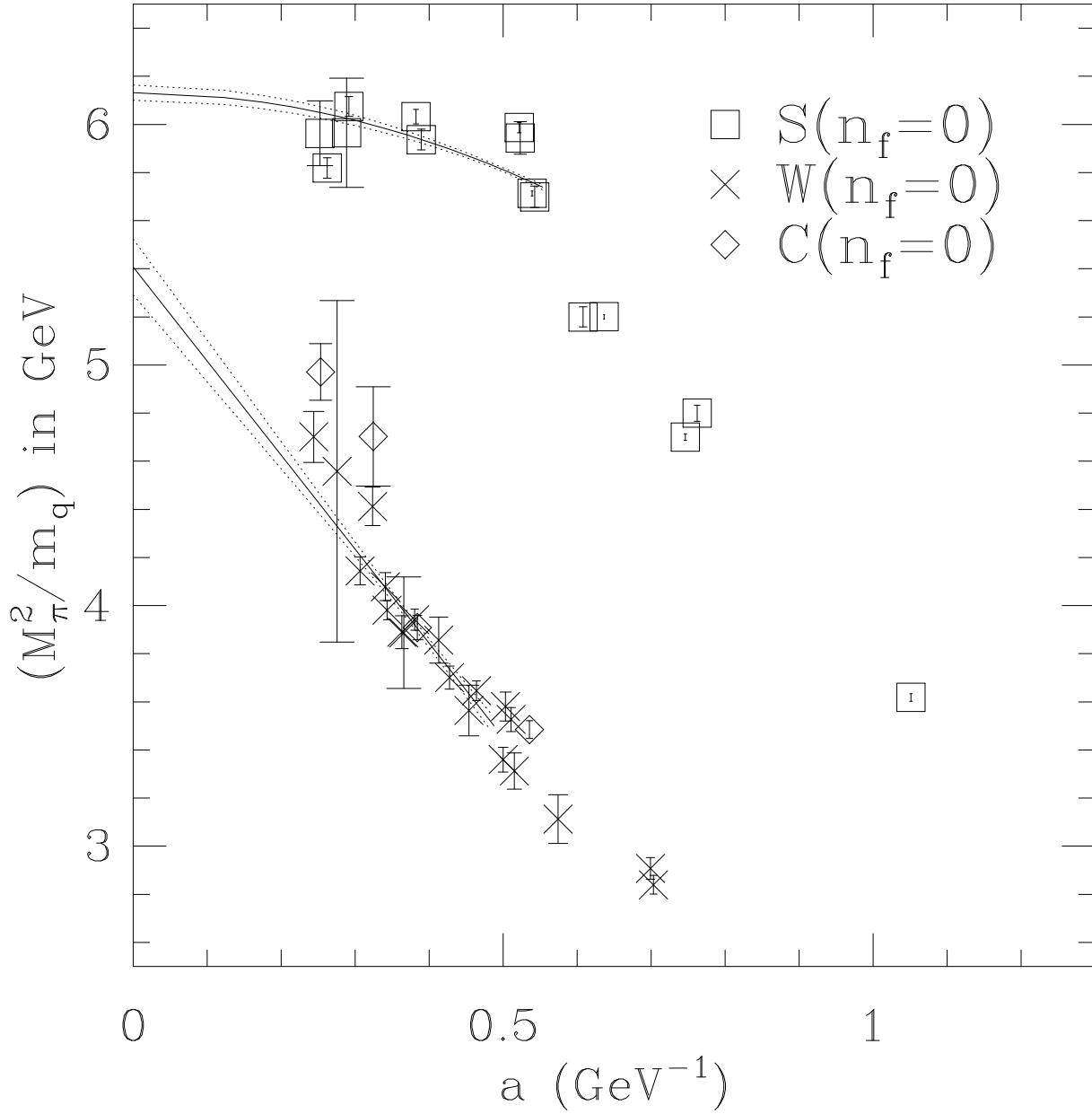


Figure 10: The slope of M_π^2 versus $m_q(\overline{MS}, 2 \text{ GeV})$ for the quenched data as a function of the lattice spacing $a(M_\rho)$. For clarity, the fit to the clover data is not shown.

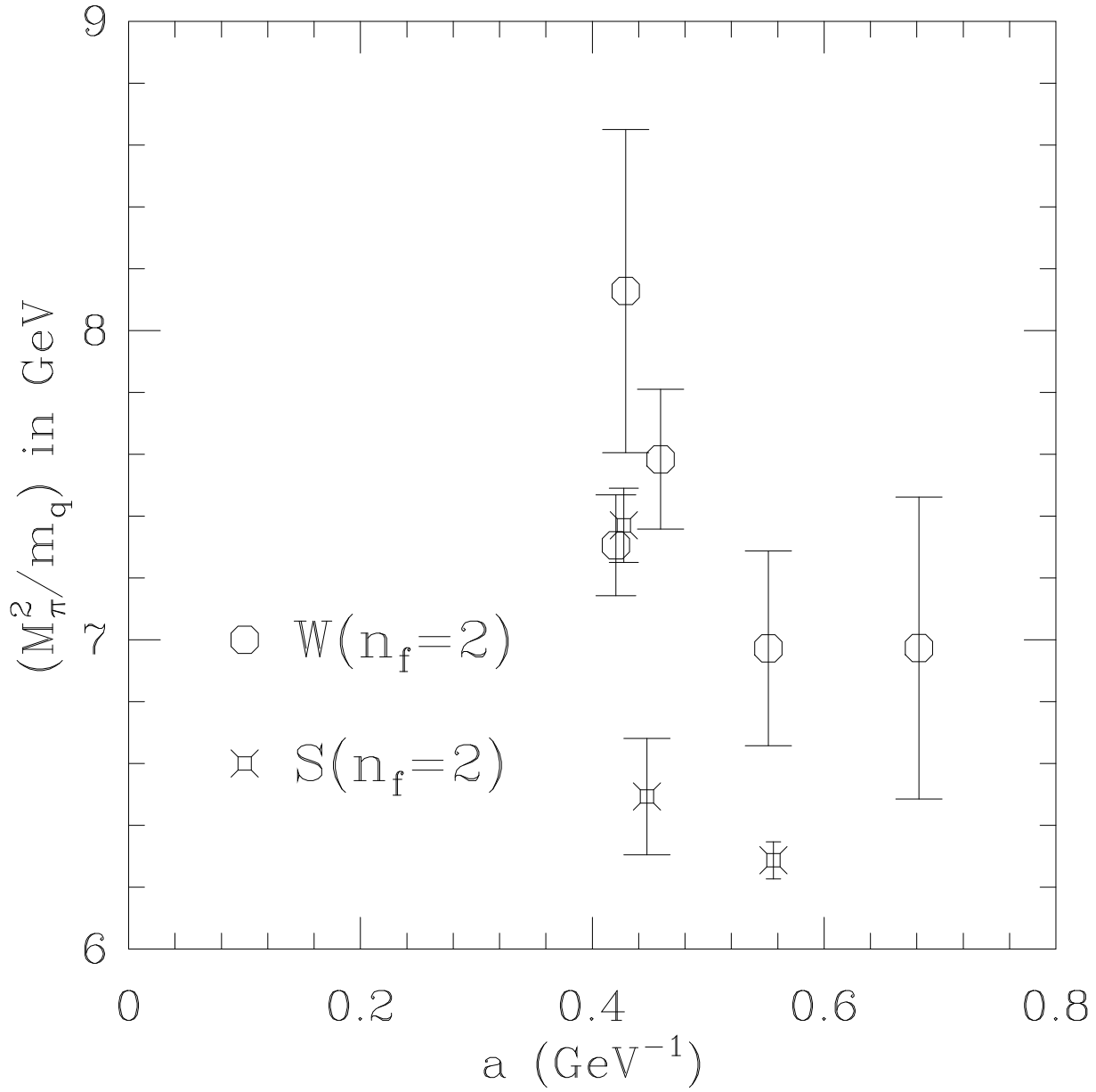


Figure 11: The slope of M_π^2 versus $m_q(\overline{MS}, 2 \text{ GeV})$ for the dynamical data as a function of the lattice spacing $a(M_\rho)$.